NASA-CR-195519

THE HYDRA DESIGN TEAM PRESENTS

THE CETACEOPTERYX

A GLOBAL RANGE MILITARY TRANSPORT AIRCRAFT

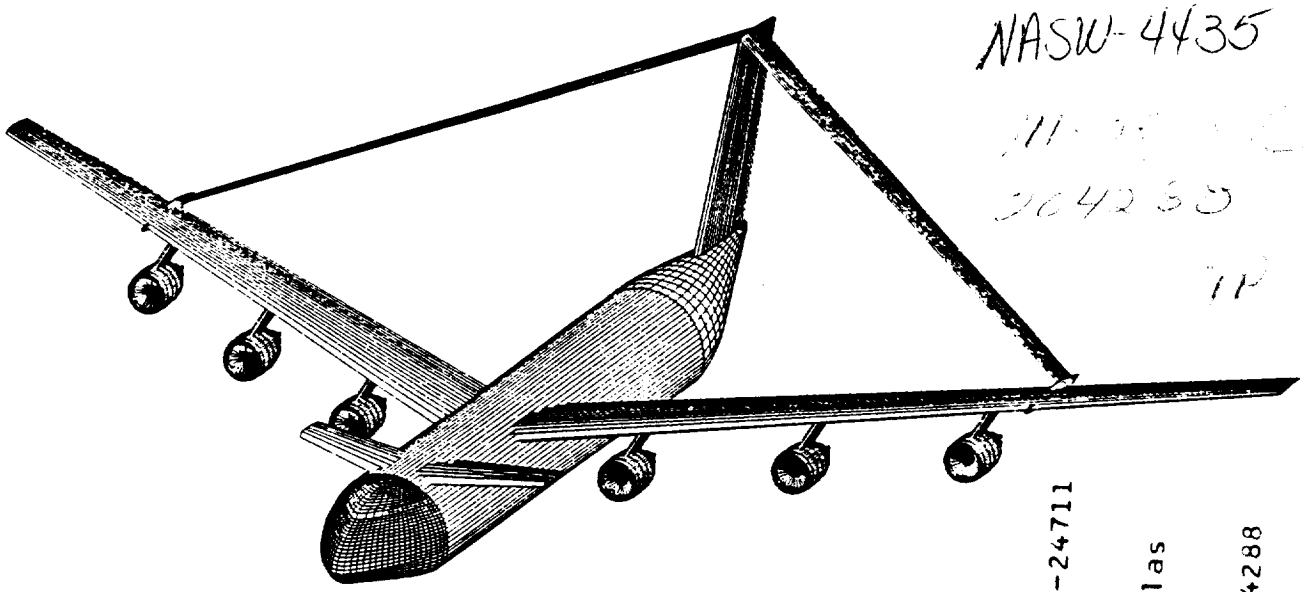

Aeronautical Engineering Department
California Polytechnic State University
San Luis Obispo, California
May 14, 1993

Hydra Design Team Members:
Chad Brivkalns
Nicole English
Tahmineh Kazemi
Kim Kopel
Seth Kroger
Ed Ortega

ABSTRACT

This paper presents a design of a military transport aircraft capable of carrying 800,000 lbs of payload from any point in the United States to any other point in the world. Such massive airlift requires aggressive use of advanced technology and a unique configuration. The *Cetaceopteryx* features a joined wing, canard and six turbofan engines. The aircraft has a cost 1.07 billion (1993) dollars each. This paper presents in detail the mission description, preliminary sizing, aircraft configuration, wing design, fuselage design, empennage design, propulsion system, landing gear design, structures, drag, stability and control, systems layout, and cost analysis of the aircraft.

STUDENT	NUMBER	SIGNATURE
CHAD BRIVKALNS	108961-00	Chad A. Brivkalns
TAHMINEH KAZEMI	109166-00	T. Kazemi
ED ORTEGA	109094-00	
SETH KROGER	108156	Seth Kroger
KIM KOPEL	104208-00	Kim Kopel
NICOLE ENGLISH	109110	Nicole English

Table of Contents

List of Figures

List of Tables

NOMENCLATURE

AR	Aspect Ratio
b_f	Front Wing Span
b_r	Rear Wing Span
cf	Equivilent Skin Friction Coefficient
cr	Wing Root Chord
ct	Wing Tip Chord
C_{Do}	Ceofficient of Drag for Steady State
$C_{D\ ih}$	Coefficient of Drag Stabalizer Incidence
C_{Dq}	Coefficient of Drag Due to Pitch Rate
C_{Du}	Coefficient of Drag Due to Speed
$C_{D\alpha}$	Coefficient of Drag Due to Angle of Attack
$C_{D\dot{\alpha}}$	Coefficient of Drag Due to Rate of Change in Angle of Attack
$C_{D\delta e}$	Coefficient of Drag Due to Elevator Deflection
C_L	Coefficient of Lift
$C_{L\ max}$	Maximum Coefficient of Lift
C_{Lo}	Coefficient of Lift for Steady State
$C_{L\ ih}$	Coefficient of Lift Stabalizer Incidence
$C_{L\ q}$	Coefficient of Lift Due to Pitch Rate
$C_{L\ u}$	Coefficient of Lift Due to Speed
$C_{L\ \alpha}$	Coefficient of Lift Due to Angle of Attack
$C_{L\ \dot{\alpha}}$	Coefficient of Lift Due to Rate of Change in Angle of Attack
$C_{L\ \delta e}$	Coefficient of Lift Due to Elevator Deflection
C_m	Coefficient of Moment for Steady State
$C_{m\ ih}$	Coefficient of Moment Due to Stabalizer Incidence
$C_{m\ q}$	Coefficient of Moment Due to Pitch Rate
$C_{m\ Tu}$	Coefficient of Moment Due to Thrust and Speed
$C_{m\ T\alpha}$	Coefficient of Moment Due Thrust and Angle of Attack
$C_{m\ u}$	Coefficient of Moment Due to Speed
$C_{m\ \alpha}$	Coefficient of Moment Due to Angle of Attack
$C_{m\ \dot{\alpha}}$	Coefficient of Moment Due to Rate of Change in Angle of Attack
$C_{m\ \delta e}$	Coefficient of Moment Due to Elevator

	Deflection
$C_{l\beta}$	Coefficient of Lift Due to Side Slip Angle
$C_{l\dot{\beta}}$	Coefficient of Lift Due to Change in Side Slip Angle
C_{lp}	Coefficient of Lift Due to Roll Rate
C_{lr}	Coefficient of Lift Due to Yaw Rate
$C_{n\beta}$	Coefficient of Yawing Moment Due to Side Slip Angle
$C_{n\dot{\beta}}$	Coefficient of Yawing Moment Due to Change in Side Slip Angle
C_{np}	Coefficient of Yawing Moment Due to Roll Rate
C_{nr}	Coefficient of Yawing Momen Due to Yaw Rate
$C_{y\beta}$	Coefficient of Side Force Due to Side Slip Angle
$C_{y\dot{\beta}}$	Coefficient of Side Force Due to Change in Side Slip Angle
C_{yp}	Coefficient of Side Force Due to Roll Rate
C_{yr}	Coefficient of Side Force Due to Yaw Rate
CG	Center of Gravity
d Cm/d Cl	Static Margin
D	Drag
e	Oswald Efficiency Factor
F	Force
g	Acceleration Due to Gravity
h	Height
l	Length
L	Lift
M	Mach Number
M_∞	Freestream Mach Number
n	Load Factor
nm	Nautical Mile
OEW	Operating Empty Weight
p	Static Pressure
q	Dynamic Pressure
S	Planform Area
T	Thrust
t/c	Thickness Ratio

Ux	Velocity in the x Direction
V	Velocity
Vy	Velocity in the y Direction
w	Width
Wz	Velocity in the z Direction
W	Weight
We	Empty Weight
Wf	Fuel Weight
Wto	Take-off Weight
W/S	Wing Loading
xcg	Longitudinal Distance to the Center of Gravity
xac	Longitudinal Distance to the Aerodynamic Center

GREEK SYMBOLS

α	Angle of Attack
α_{nac}	Nacelle Angle of Attack
b	Side Slip Angle
Γ	Circulation
Γ	Wing Dihedral
λ	Taper Ratio
Λ	Wing Sweep
ζ_{p}	Long-period (Phugoid) Damping Ratio
ζ_{sp}	Short-period Damping Ratio
ζ_{spiral}	Spiral Damping Ratio
ζ_{roll}	Roll Damping Ratio
ρ	Density
ω_{p}	Long-period (Phugoid) Damping Frequency
ω_{sp}	Short-period Damping Frequency
ω_{DR}	Dutch Roll Damping Frequency

INTRODUCTION

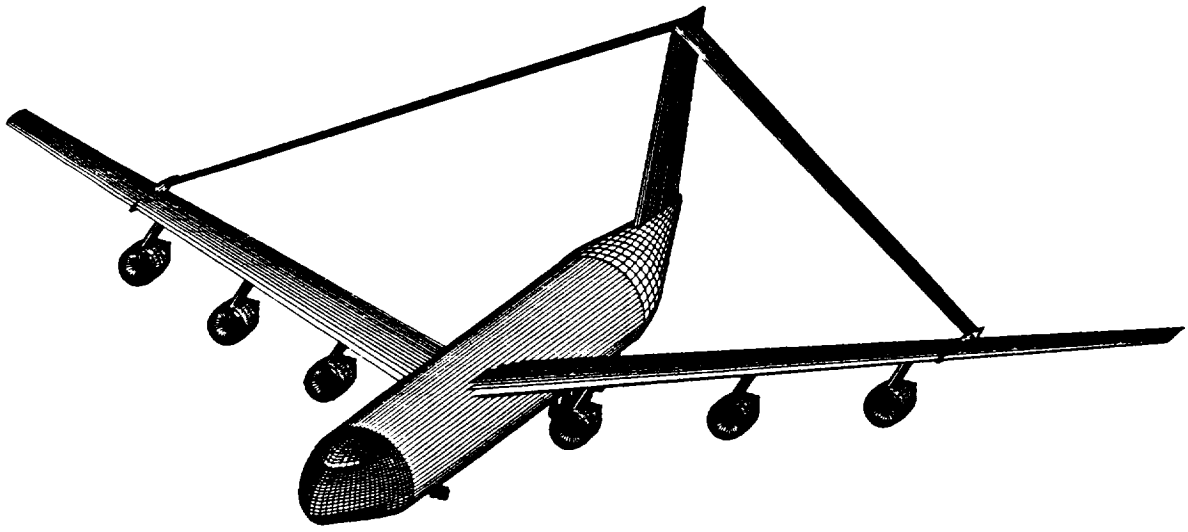

1. INTRODUCTION

During periods of armed conflict or international emergencies, a military's capability to airlift troops, equipment, and other cargo quickly and efficiently is of prime importance. However, recent developments - namely the end of the cold war - have caused the military to reevaluate nearly every aspect of its mission, strength and readiness. For instance, there are no longer pressing reasons to maintain a sustained military presence in foreign countries. Similarly, foreign countries are becoming increasingly hostile towards the idea of allowing a United States military presence on their soil, as exemplified by the refusal of the Philippines to renew the leases of several critical American bases. Operationally, this means that the United States cannot count on logistics support, such as refueling, during airlift operations. In addition, the military's responsibilities are expanding to include domestic and international humanitarian relief efforts, as demonstrated in the Somalian famine relief operations and aid to victims of the hurricanes which recently ravaged Florida and Hawaii.

In order to meet the future needs of a military faced with these challenges, the design of a high capacity strategic airlifter capable of carrying large amounts of cargo globally without refueling becomes necessary. The Hydra team's *Cetaceopteryx* is such an aircraft.

A strategic cargo aircraft, like the *Ceteaceopteryx*, follows a much different philosophy than a tactical airlift aircraft, such as the McDonnell Douglas C-17. The McDonnell Douglas C-17 is capable of fulfilling a wide variety of

missions. It is capable of delivering personnel and supplies close to a battle front, and has the capability to perform paratroop drops. It is, like the *Cetaceopteryx*, capable of transporting cargo globally, but only with aerial refueling. The McDonnell Douglas C-17 also has the unique ability to transport its cargo from its home base directly to a tactical theater without the intermediate stops required by Lockheed's C-141 and C-5. During current airlift operations, cargo must first be delivered to a strategic airbase, and off-loaded to smaller cargo aircraft such as Lockheed's C-141 and C-130 to be transported to the battle field. For the Air Force, this new system represents savings in both money and person-hours (as opposed to man-hours). However, using the McDonnell Douglas C-17 in this manner is only advantageous if a well prepared network of tankers exists to perform mid-air refueling. With the possibility of maintaining such a network in the future uncertain, the attractiveness of a global range military transport, like the *Cetaceopteryx*, becomes obvious. When coupled with the additional savings in person-hours and fuel that accompanies such an operationally independent aircraft, the logic of adopting an aircraft like the *Cetaceopteryx* becomes evident.

The *Cetaceopteryx* is unique in its capability to transport 800,000 pounds of cargo - nearly three times the capacity of the Lockheed C-5 - globally without refueling. Given this unique ability, many unique design decisions had to be made. The most obvious is the joined wing configuration which possesses many aerodynamic, structural and weight advantages as compared to a conventional cantilever wing aircraft. The weight savings is of critical importance with respect to fuel efficiency, one of our driving design constraints.

In addition, advanced composites are used for the primary structural material rather than conventional metals and their derivatives. While no current cargo aircraft uses more than a few composite components, Hydra feels that the technology available at the *Cetaceopteryx's* service entry date (2015) will allow the production of a primarily composite aircraft. While the cost of such an aircraft is high, it must be recognized that no other aircraft with these capabilities exists.

MISSION PROFILE

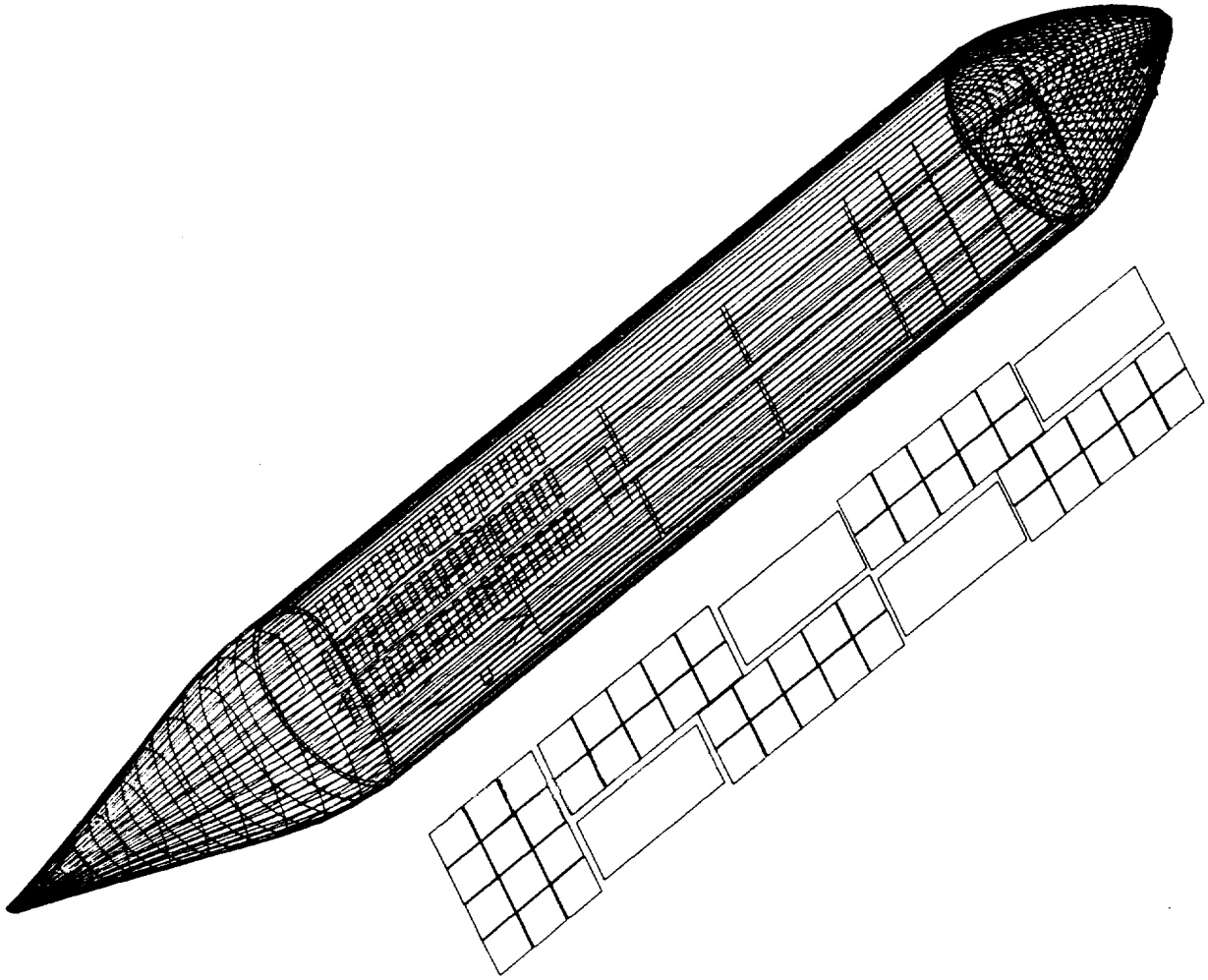

2. MISSION PROFILE

There are two different mission profiles the *Cetaceopteryx* is required to perform: the primary and secondary missions.[1] Both missions involve transporting large amounts of cargo over long ranges and returning to home base without refueling.

2.1. Primary Mission

The primary mission involves transporting the maximum required payload (800,000 lbs) a distance of 6,500 nautical miles, at which point the cargo is off-loaded and replaced with a load of 120,000 lbs (15 percent of maximum payload). The aircraft is then required to return 6,500 nautical miles to its home base. This mission is to be carried out without refueling. Table 2.1.1 summarizes the *Cetaceopteryx's* primary mission.

Table 2.1.1 - Primary Mission

Total Range	13,000 nm
First Leg Range	6,500 nm
First Leg Payload	800,000 lb
Second Leg Range	6,500 nm
Second Leg Payload	120,000 lb

2.2. Secondary Mission

The secondary mission entails transporting a payload of 600,000 lbs a distance of 8,400 nautical miles, at which point the aircraft is completely unloaded. The aircraft is then required to return 8,400 nautical miles to its home base, again without refueling. Table 2.2.1 summarizes the *Cetaceopteryx's* secondary mission.

Table 2.2.1 - Secondary Mission

Total Range	16,800 nm
First Leg Range	8,400 nm
First Leg Payload	600,000 lb
Second Leg Range	8,400 nm
Second Leg Payload	0 lb

2.3. Strategic vs. Tactical Airlift

The *Cetaceopteryx* is a strategic airlifter, tasked with carrying large payloads to an airfield near the desired military theater at which point its cargo is off loaded and distributed to smaller tactical airlifters. The *Cetaceopteryx* does not have the ability to perform missions such as paratroop drops, Low Altitude Parachute Extraction System (LAPES) drops, and is not intended to venture into the tactical theater itself. Since the *Cetaceopteryx* is a very large and expensive aircraft, with a commensurately valuable payload, the risk of operating such a resource in a hostile environment cannot be justified.

PRELIMINARY SIZING

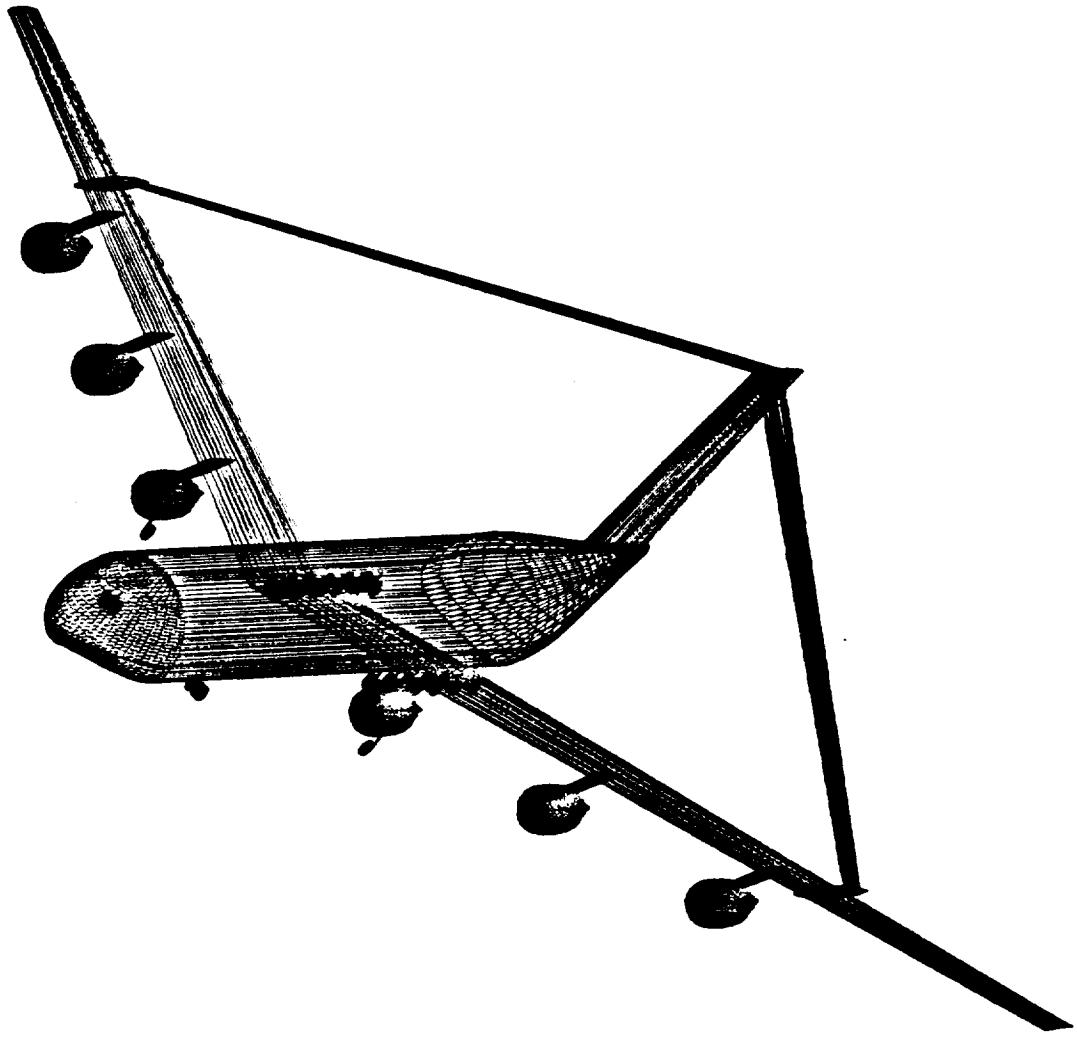

3. PRELIMINARY SIZING

As has been noted, the *Cetaceopteryx* is larger than any existing aircraft, with a gross takeoff weight of 2,140,000 lbs. The next largest operational aircraft is the Russian Antonov An-225 Cossack, a military cargo aircraft with a maximum takeoff weight of 1,300,000 lbs.

The *Cetaceopteryx's* weight was derived by the methods presented in Reference 2. The gross take-off weight was calculated from the addition of fuel weight, the operating empty weight, and payload weight.

Wto = 2,140,000 lbs

Wf = 890,000 lbs

OWE = 450,000 lbs

We = 444,000 lbs

These weights were arrived at based on the assumptions of a cruise lift to drag ratio (L/D) of 29 and a specific fuel consumption (SFC) of 0.45 lbm/lbf-hr. Although these numbers may seem optimistic, justification is provided in the aerodynamics, drag, and propulsion sections.

Figure 3.0.1 shows the graph of the *Cetaceopteryx's* take-off thrust-to-weight vs. wing loading, from which the following design point was selected:

T/W = 0.29

W/S = 164 lb/ft^2

At this point, the C_{Lmax} 's required for take-off and landing are 2.1 and 2.45, respectively.

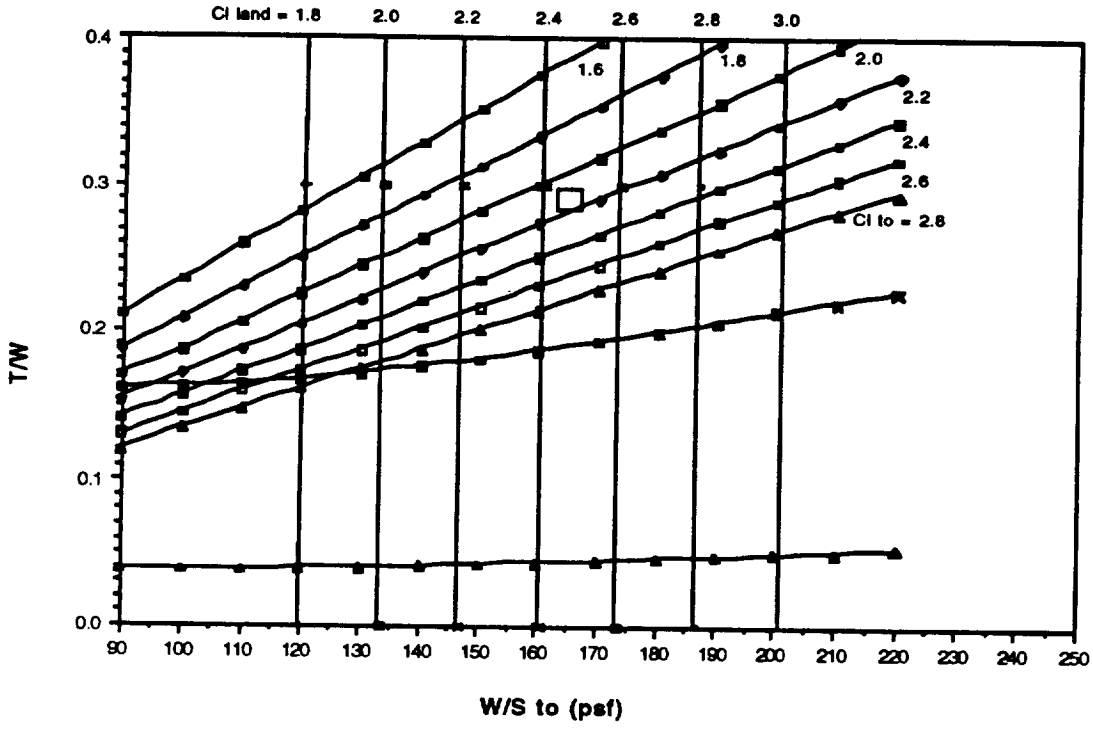

Figure 3.0.1 - Thrust to Weight vs. Wing Loading

Given these values of take-off and landing C_{Lmax} , the *Cetaceopteryx's* wing area was determined to be 12,363 ft^2 with a total take-off thrust of 620,600 lbs. The thrust to weight ratio posed a major constraint in selecting this design point. This value was required to provide desirable performance, while not exceeding the *Cetaceopteryx's* technology availability date of 2010.

AIRCRAFT CONFIGURATION

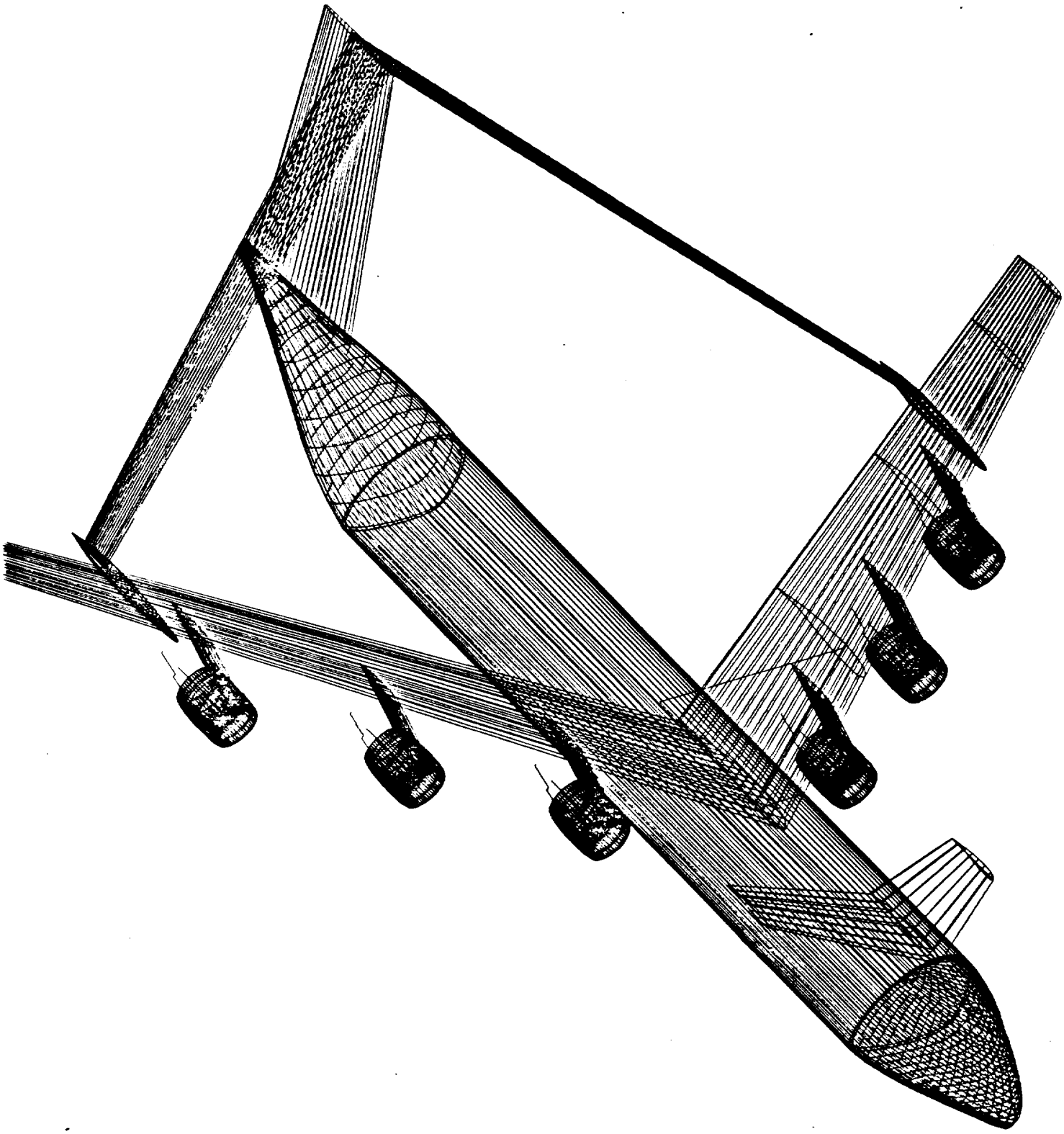

4. AIRCRAFT CONFIGURATION

4.1. Wing

Invented and developed extensively by the late Dr. Julian Wolkovitch (Ph.D.), the joined- wing configuration is comprised of moderately dihedralled, aft-swept front wings that are structurally connected to heavily anhedralled, forward-swept rear wings. The result, as is shown in Figure 4.1.1, is essentially a diamond structure in both the front and plan view, which enables the wings to brace one another in both the vertical and longitudinal planes.

As noted earlier, the primary and secondary mission requirements for the Cetaceopteryx specify the transportation of heavy payloads over extremely long ranges. A design that maximizes aerodynamic efficiency (high Oswald's efficiency factor and high L/D) and minimizes structural weight (high strength-to-weight ratio) is, in this case, of paramount importance; it would be impossible to meet the mission requirements without them. However, high aerodynamic efficiency and low weight are not original or unique design goals -- nearly every modern aircraft has been designed with these two criteria in mind. In this case, though, these demands require a unique solution.

Initially, three principal configurations were analyzed and compared: 1) conventional aft-swept wing; 2) forward-swept wing; and, 3) joined-wing. While a great deal of information, both theoretical and empirical, is available for the conventional arrangement, its applicability to the design of a global range military transport is limited by the fact that, as its aspect ratio is increased in order to increase

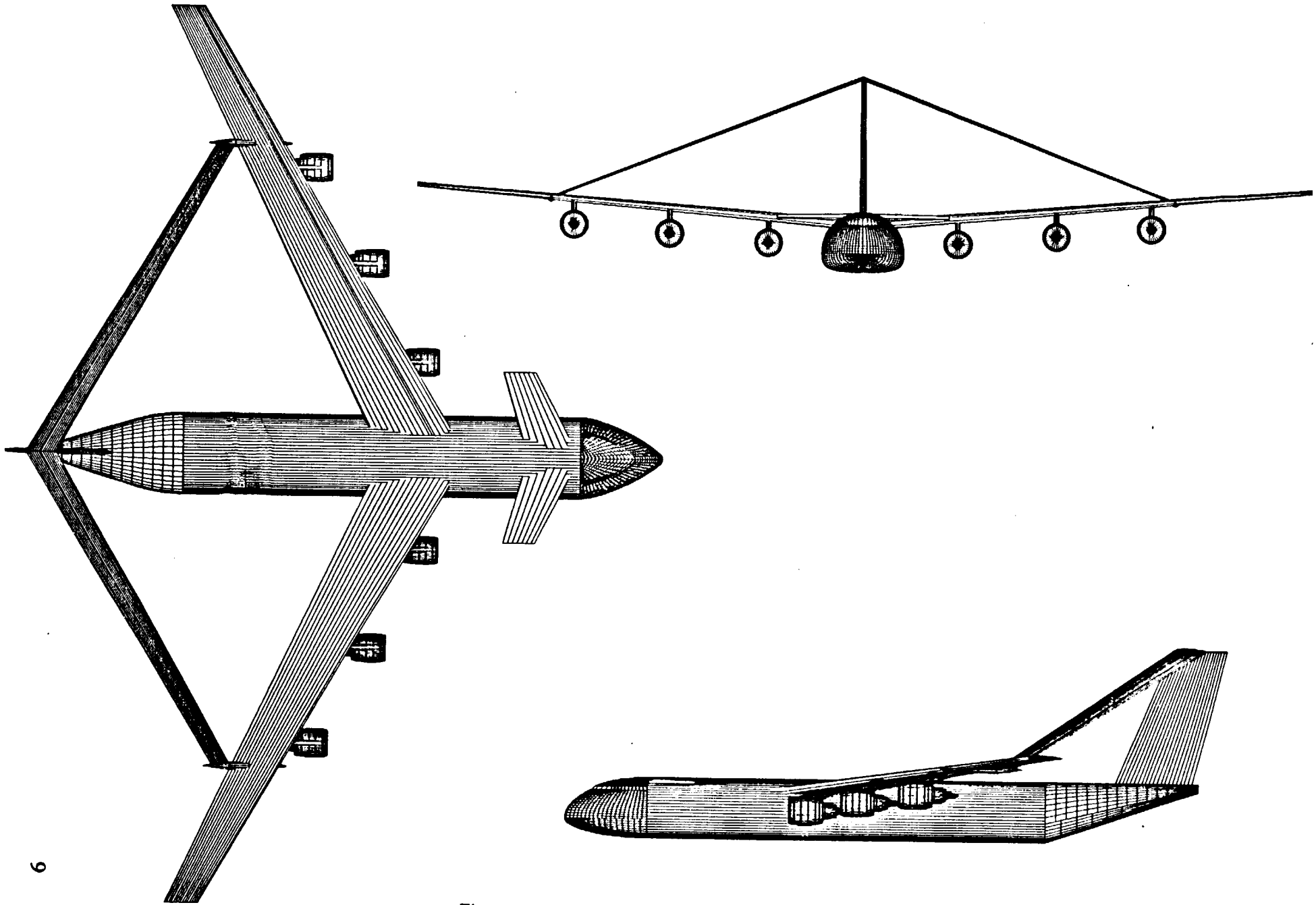

Figure 4.1.1 - Cetaceopteryx Three View

aerodynamic efficiency (reduce induced drag), its structural efficiency decreases unacceptably. In other words, the additional structure required to resist the forces and moments in the outer wing panels results in a disproportionately large weight increase.

A similar situation exists for the forward-swept configuration. Because the tip vortices are inherently weaker for this design (flow over the wing tends to flow towards the root, rather than towards the tip as it does for an aft-swept planform), it has an inherent aerodynamic advantage over the conventional wing. This performance gain is mitigated, however, by the fact that the forward-swept wing exhibits structural divergence at even low aspect ratios; to date, the forward-swept wing demonstrators that have been built have been small (fighter-sized) aircraft with low aspect ratio wings. In addition, composite construction was required to successfully combat the structural divergence problem.

The joined-wing, on the other hand, is capable of high aerodynamic efficiency with an accompanied weight *savings*, a result of the mutual bracing that the front and rear wings provide one another. Several studies (References 3, 4, and 5) have shown that, when compared to conventional configurations that are aerodynamically equivalent -- that is, configurations having equal gross projected areas, taper ratios, sweep angle magnitudes, and front/rear lifting surface area ratios -- the joined-wing design is generally from 65 percent to 78 percent of the cantilever wing-and-tail's weight. This weight reduction stems from the fact that, for the joined-wing, the bending axis of the front and rear wing combination is a plane

through the neutral axes of the front and rear wings (Figure 4.1.2).

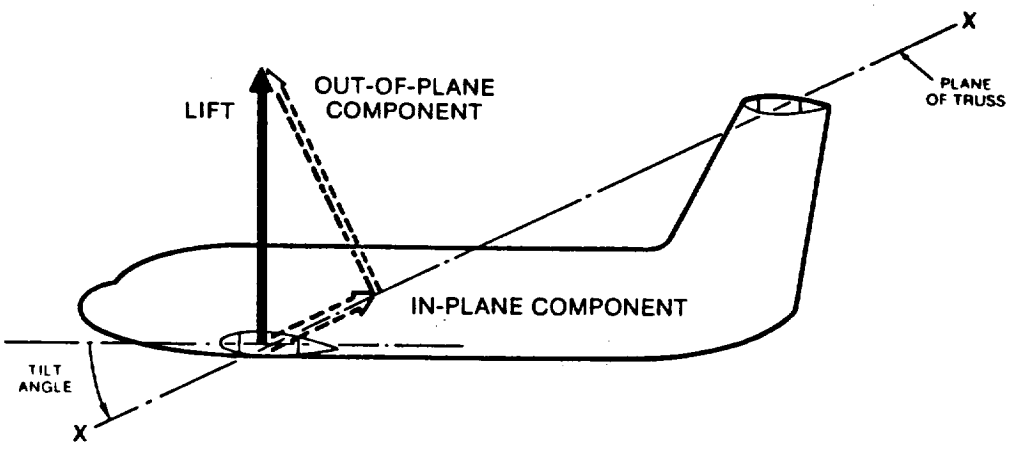

Figure 4.1.2 - Bending Axis Of Joined Wing

As can be seen, the lift generated by the wings may be decomposed into two components: one parallel to the bending axis ("inplane"), and one perpendicular to it ("out-of-plane"). The wing's truss structure effectively dissipates the inplane load component, and the out-of-plane component -- which is less than the load component resisted by a conventional cantilever wing -- is dealt with through the judicious distribution of material in the wing's box structure.[4] In order to obtain the maximum moment of inertia about the bending axis, structural material must be concentrated in the upper leading edge and lower trailing edges of the wingbox (Figure 4.1.3). The wingbox itself, which for a conventional wing typically occupies the region between 15 percent and 65 percent of the wing chord, may be expanded outwards along the chord so that it extends from 5 percent to 75 percent of the wing's chord.[4] A visual

comparison of cantilever versus joined wingbox construction is provided in Figure 4.1.4.

SHADED REGION INDICATES EQUIVALENT SKIN THICKNESS,
ie: AVERAGE OF LOCAL SKINS, STRINGERS AND SPARS.
EQUIVALENT SKIN THICKNESS IS EXAGGERATED FOR
CLARITY, TO EMPHASIZE THE TAPER.

Figure 4.1.3 - Asymmetrical Wing Box

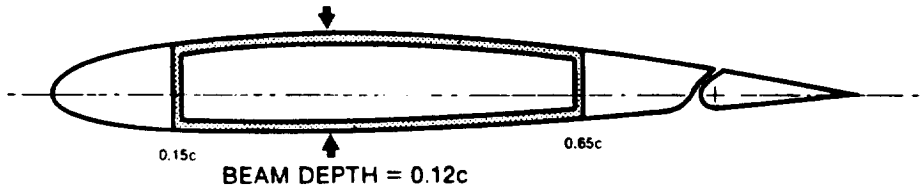

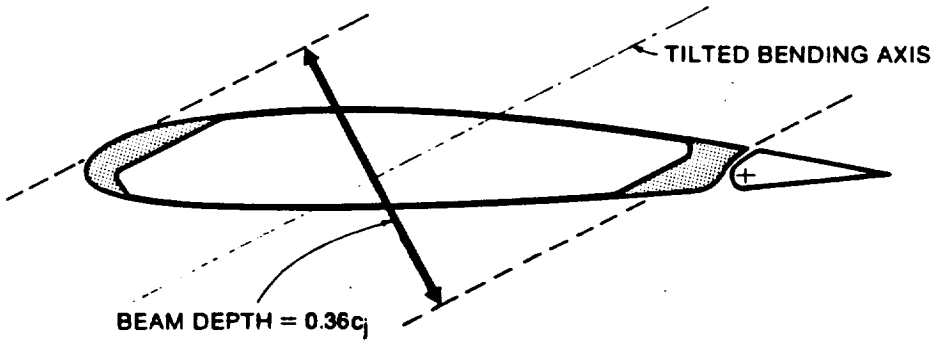

Figure 4.1.4 - Wing Box Comparison

The primary advantages of the joined-wing, then, are threefold: 1) the wing structure may be constructed lighter than an aerodynamically equivalent cantilever wing-tail configuration; 2) wings of higher-than-normal aspect ratio, which would be structurally unfeasible if of cantilever construction, may be used with corresponding increases in aerodynamic efficiency (reductions in induced drag); and 3) the elongated wingbox structure allows for an increase in fuel storage within the wings.[4]

The increase in fuel volume is a function of two factors -- the increase in wing box cross-sectional area caused by relocating the fore and aft wing spars outward (relative to the airfoil centroid), and the fact that more span is available (with the front *and* rear wings) to carry fuel. Figure 4.1.5 graphically represents this enhanced fuel storage capability by comparing a conventional and two joined-wing configurations of equal span, planform area, and airfoil thickness; the cantilever aircraft is used as the baseline for the comparison. Both joined-wing configurations demonstrate a significant increase in fuel capacity, with the inboard-jointed version offering the most additional fuel volume (54 percent more than the cantilever structure, 32 percent more than the tip-jointed configuration).

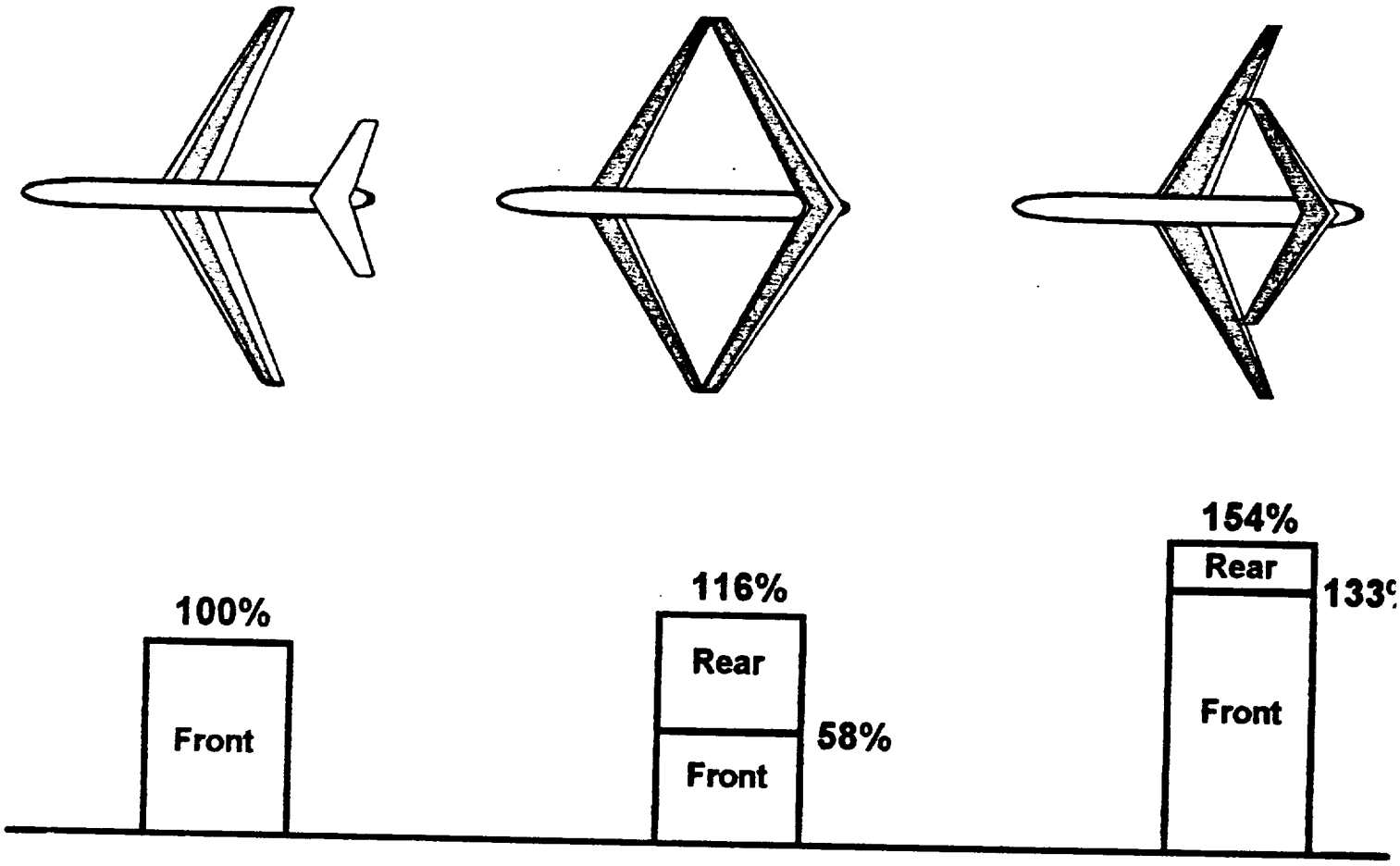

Figure 4.1.5 - Fuel Storage Volume

Other advantages of the configuration include [5]

1. High stiffness
2. Good transonic area distribution
3. High trimmed $C_{L_{max}}$
4. Reduced wetted area and parasite drag
5. Capability for direct lift control (the ability to create a pure lift force without pitching the aircraft)

6. Capability for direct sideforce control (the ability to create a pure sideforce without yawing the aircraft)

7. Good stability and control characteristics

Direct lift and sideforce capability, derived from coordinated deflections of the wing's front and rear control surfaces (Figure 4.1.6), is potentially of great value for a large military transport. In a crosswind landing situation, for example, the aircraft would be able to use direct sideforce to counter the lateral component of wind velocity while maintaining its alignment with the runway (no "crabbing" into the wind), thus reducing the tire sideloading on touchdown. During takeoff, direct lift could be used to reduce the amount of rotation required.

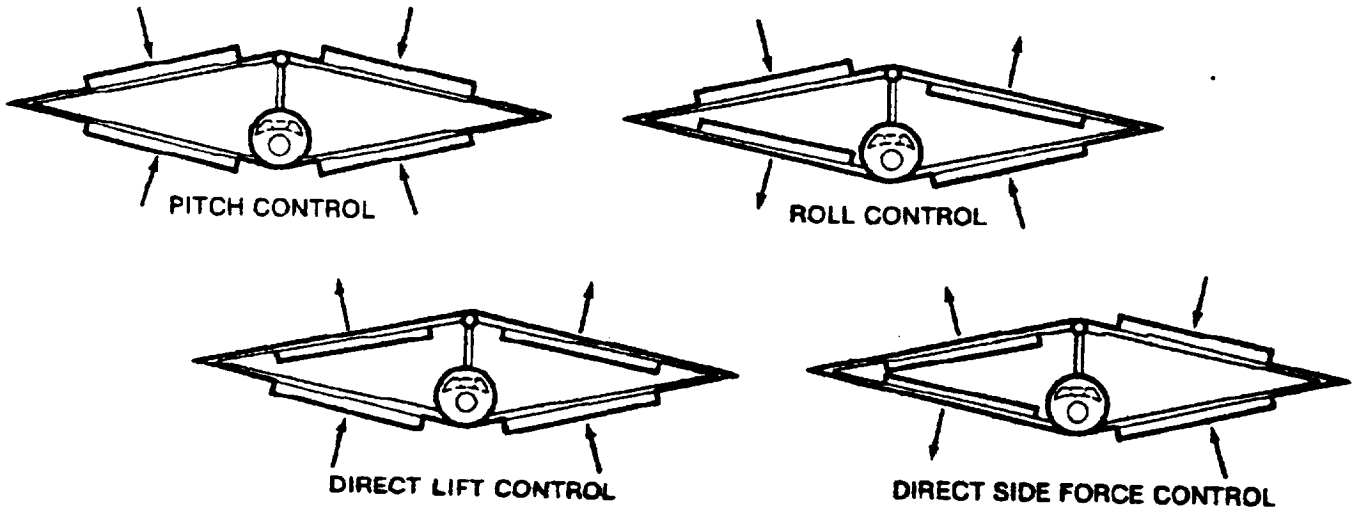

Figure 4.1.6 - Control Surfaces

It can be seen, then, that the joined-wing is an aerodynamically efficient, lightweight configuration suitable for use on a long-range transport aircraft.

The joined-wing is not a panacea, however. An infinite number of configuration possibilities exist, with variations in the dihedral, anhedral, sweep, and joint location only a few of the many factors differentiating them. Optimum aerodynamic and/or structural performance is only obtained by careful design and attentive manipulation of several important parameters.

One of the most important variables in joined wing design is the spanwise location of the point where the front and rear wings join. Several studies have analyzed the joined wing configuration with span ratios of from 0.3 to 1.0, where the span ratio is defined as the ratio of rear to front wing span.[4] The results of these studies indicate the following:

1. Optimum aerodynamic performance is obtained with a tip-jointed configuration (span ratio equal to 1.0)

2. The lowest structural weight is obtained if the joint is located at a span ratio of 0.7.

In the case of the tip-jointed arrangement, the aerodynamic advantages consist of a higher span efficiency factor, suitability for winglets, and greater trimming moment capability -- for equal forward and rearward sweep, a design with a span ratio of 1.0 locates the trimming surfaces of the rear wing further from the center of gravity than a design with an inboard joint location, thus providing the maximum pitching moment possible for a

joined wing design. However, a tip-jointed design also proves to be structurally heavier than an aerodynamically equivalent cantilever wing-and-tail design.[5]

The opposite is true in the case where the rear-to-front wing span ratio is 0.7. Wolkovitch and others have shown that this configuration provides the greatest weight savings over a conventional cantilever wing/tail design while maintaining an advantage in aerodynamic efficiency. Compared to the tip-jointed arrangement, the inboard-joined configuration offers a significantly lower span efficiency factor, yet it still, on average, produces two to three percent better efficiency than an aerodynamically equivalent conventional design.

The question naturally arises, then, as to which is preferable: an extremely light structure that provides aerodynamic efficiencies above the norm, or a slightly heavier-than-average structure that provides much better aerodynamic performance. However, this in turn leads to another question, one concerning the nature of the rear wing: is the rear wing used to produce lift, or is it used only as a brace for the front wing? While at first it might seem very desirable to use the rear wing as a lifting surface to maximize the total lift, doing so can result in an unstable aircraft as the aerodynamic center shifts rearward. The alternative, then, is to use the rear wing as a bracing strut that carries, hopefully, little or no download to trim the aircraft -- in essence, a strut that does double duty as a control surface.

Given this choice, Hydra opted to use the latter approach for two very important reasons. First, while the General Dynamics F-16 Flying Falcon and the Grumman X-29

Forward Swept Wing Flight Test Demonstrator have shown that unstable planes can be made controllable through fly-by-wire control systems, these aircraft differ significantly from the *Cetaceopteryx* in both size and maneuverability. The problem of moving very large control surfaces rapidly enough to ensure that the aircraft remain stable and controllable could well prove to be impossible. Second, by assuming that the wing and tail, despite their unique configurations, act in a conventional manner -- the front wing providing lift and the rear used for trim purposes -- the design and analysis of the aircraft could proceed from a known point of departure. In this way, the structural rigidity of the joined-wing configuration could be exploited to support a front wing of higher-than-normal aspect ratio (for optimum aerodynamic performance), while the principles guiding the design would not be unduly abstract.

Following this design philosophy, the *Cetaceopteryx* is in many ways modeled after contemporary military airlifters such as the McDonnell Douglas C-17 and Lockheed's C-5 Galaxy and C-141 Starlifter. For instance, the front wing is mounted high on the fuselage, despite the fact that this yields non-optimal dihedral and anhedral values (5 and 20.84 degrees, respectively), with the ideal values being 10 and 30 degrees (Reference 6). This apparent design imperfection is a concession to two factors: 1) the need to place the engines in a position where they would be easily accessible for maintenance and replacement; and 2) the desire to constrain the vertical tail to a "reasonable" height.

Had the front wing been placed in a lower position, engine location would have become a critical problem, since the alternative mounting points -- beneath the rear wing, and

above the front wing -- have serious shortcomings. If the powerplants had been suspended from the rear wing, the aircraft would have experienced excessive nose-down pitching moment during takeoff and routine engine maintenance would have been rendered nearly impossible by their height above the ground. Mounting the powerplants above the wings would also have caused problems. In the event of critical engine damage or the need to cannibalize an aircraft for parts in an area of the world where the aircraft's normal maintenance facilities were unavailable, the technical difficulties involved in removing an engine from above the wing, particularly from the outboard sections where the wing -- due to dihedral -- is highest, would have been significant.

In addition, the dihedral and anhedral of the front and rear wings is also limited by the desire to keep the size of the vertical tail as small, within practical bounds, as possible. On the ramp, the root of the rear wing is 90 feet above the ground. Given the number of actuators and mechanisms required to power the rear wing mounted elevators, this is a considerable height at which to perform extensive maintenance, particularly if work should be required at an intermediate airfield where the specialized facilities available at the aircraft's home field do not exist. If the optimum 30 degree anhedral is used (and the front wing dihedral remains at the baseline 5 degrees), the overall height increases to over 128 feet, a 43 percent increase; if the optimum dihedral is used as well, the height becomes 146 feet, a net increase in vertical distance (over the baseline) of 63 percent.

In general, the most important limitation of the joined-wing configuration lies in pitch control. Because the front

and rear wings must be physically connected, the location of the rear wing relative to the center of gravity and front wing is constrained; consequently, the pitching moment generated by the rear wing (in its capacity as horizontal tail) is also constrained. In response, several courses of action are available.

First, if the sweeps of the front and rear wings are to be held constant, the front-rear wing-joint location may be moved outwards toward the front wing tip. As noted earlier, however, the structural weight of the entire assembly will also be increased. Furthermore, if it is desired to hold the anhedral of the rear wing constant, the height of the vertical tail will increase proportionately, which is, as has been shown in *Cetaceopteryx's* case, unacceptable.

Second, the sweep of the front wing may be increased. This, too, has several negative side-effects: the wing's lift curve slope is reduced, the maximum lift coefficient of the wing decreases, the aerodynamic center moves aft, and, again, structural weight increases (Reference 6, 7). If all parameters are held constant aside form the front wing's sweep, the aircraft's center of gravity will also move aft; in effect, the tail moment arm will not increase as much as was anticipated.

Finally, the sweep of the rear wing may be increased. For this case, the principal drawback is of a structural nature. Since it acts not only as a control surface (a horizontal tail) but as a brace, the rear wing must be able to resist the compressive load from the front wing without buckling. However, if the design is constrained to a particular front-to-rear area ratio, increasing the rear wing's sweep results

in a weight increase that stems not only from the addition of material to lengthen the wing but also from the addition of material required to resist buckling. If, on the other hand, the front-to-rear area ratio is not constrained (the rear wing is allowed to vary in aspect ratio), the structural weight of the rear wing again increases in order to prevent buckling.

Hydra, however, chose to correct the joined-wing pitching moment limitations in a different manner. Rather than compromising *Cetaceopteryx's* aerodynamic and structural properties by manipulating the sweep angles or joint location -- all of which would increase the weight -- Hydra located a low aspect ratio canard ahead of the front wing to provide pitch control for rotation and cruise trim.

4.2. Canard

In wind tunnel tests of a joined-wing cruise missile design, Wolkovitch noted (Reference 7) that the addition of a canard provided several major benefits to the configuration's performance: 1) enhanced pitch control; 2) increased C_{Lmax} ; and 3) the ability to trim over a wide range of center-of-gravity locations with no significant loss of maximum lift.

The increased C_{Lmax} results from the fact that the leading edge vortex shed from the canard induces considerable augmentation of the front wing's lift. In a comparison between three configurations -- conventional cantilever, joined-wing, and joined-wing with canard -- where the values of C_L were referred to the total exposed lifting surface area of the applicable design, Wolkovitch measured C_L values that were four to seven percent (joined-wing) and more than nineteen percent (joined-wing with canard)

higher than the conventional configuration. In the case of the canard-equipped model, the C_L versus angle of attack graph was still rising at 22 degrees, the highest angle of attack tested. For a large, joined-wing aircraft required to efficiently transport heavy loads long ranges -- such as the *Cetaceopteryx* -- the addition of a canard is of great benefit.

In addition, the gains in C_L mentioned above were maintained over a wide range of stable static margins; in other words, the center of gravity location had little effect on the canard's ability to enhance the joined-wing's trimmed cruise performance. For a military airlifter expected to encounter a wide variety of loading configurations, this feature is of prime importance.

As can be seen, the canard offers *Cetaceopteryx* more than just enhanced pitch moment capability. However, setting these additional benefits aside, adding a canard also increases the aircraft's structural weight. Compared to altering the wing-joint location or altering the front or rear wing sweep angles, though, the canard is the lighter alternative, as the joined-wing only configurations are approximately ten to fifteen percent heavier.

The canard also serves in the highly non-aerodynamic role of speedbrake during landing rollout. To accomplish this, the upper and lower surfaces are hinged so that, upon touchdown, they may be hydraulically extended to present approximately 1000 square feet of equivalent flat plate area to the oncoming flow.

4.3. Fuselage

The configuration of the fuselage was essentially determined by the cargo volume requirement, which stipulated that the aircraft be capable of carrying the volumetric equivalent of six M-1 main battle tanks, three AH-1G attack helicopters, twenty 463L pallets, and 200 combat troops. The total weight of this equipment combination is, however, in excess of the 800,000 pound maximum payload specified in the request for proposal, which leads to the undesirable situations of: a) the aircraft operating with maximum payload and a partially empty cargo bay; and b) the aircraft operating with a full cargo bay but with less than maximum design payload.

For military operations, it is not enough to carry large amounts of cargo great distances; the cargo must also be offloaded as rapidly as possible and new cargo (if it is to be carried) loaded equally as rapidly. In order to minimize the amount of time thaat the *Cetaceopteryx* spends on the ground involved in the logistics of cargo transfer, the aircraft is configured with a tail hatch/door and an upward-hinged nose (similar to the Lockheed C-5 Galaxy) with an extendable ramp that allows simultaneous loading and unloading of cargo from either end of the fuselage.

The landing gear is located external to the lower corners of the fuselage in aerodynamic pods, rotating to place the wheel rotation axes parallel to the fuselage's longitudinal axis upon retraction. Due to lack of space beneath the main cargo bay, the nose gear is separated into two assemblies located along the side of the fuselage, with the net effect of producing, in conjunction with the slightly wider-tracked main gear (twelve bogies), a hybrid tandem/conventional

configuration. In order to decrease the possibility of tipover in crosswinds or while turning, small outrigger gears are provided that retract into the inboard engine nacelles.

WING DESIGN

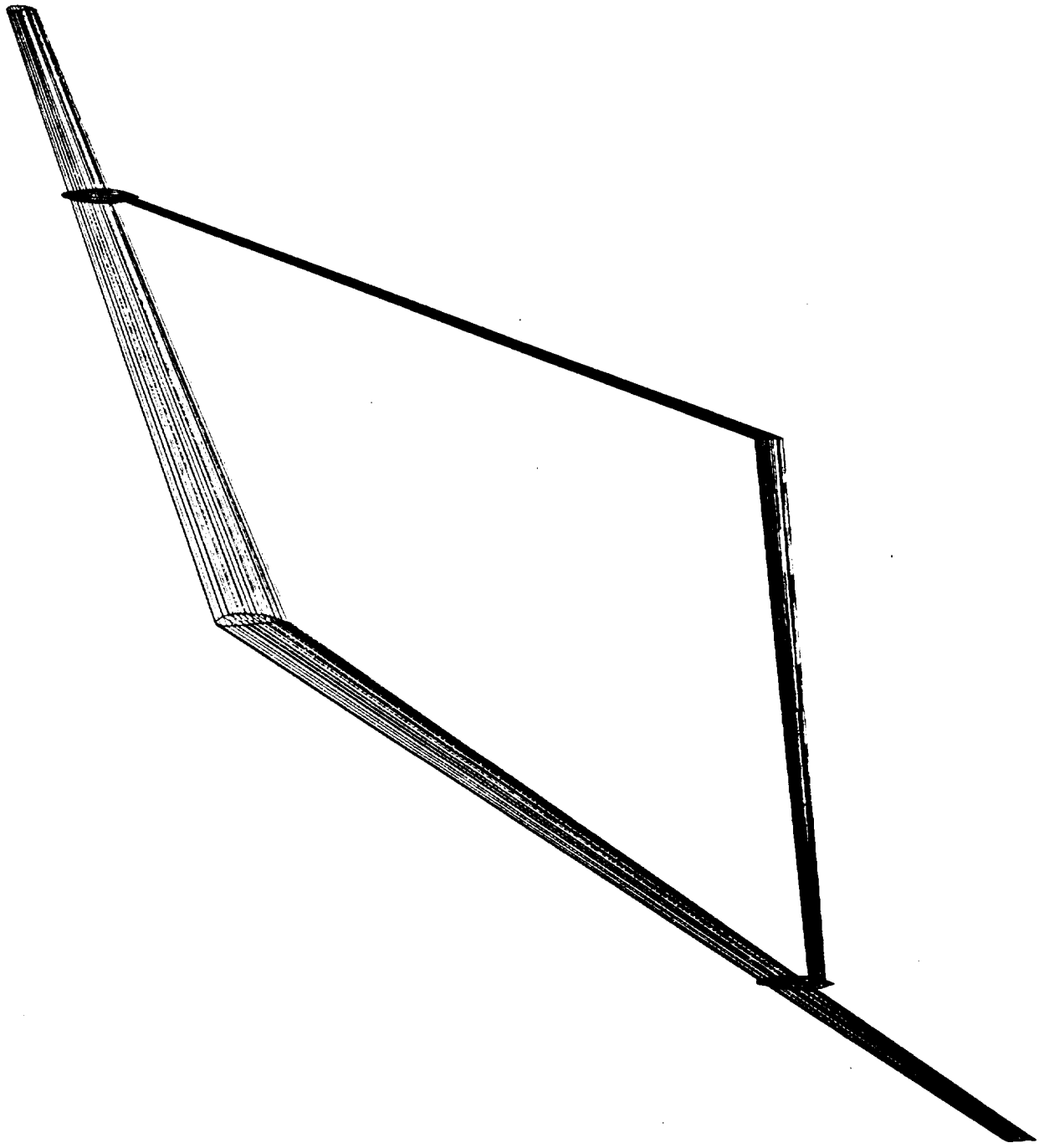

5. WING DESIGN

The *Cetaceopteryx* is a joined wing concept with two major lifting surfaces: a forward swept anhedral rear wing that originates at the tip of the vertical tail and attached to the aft swept dihedral front wing. The front wing is a high wing originating at approximately one third of the fuselage length and reaching outward at a thirty degree sweep to an overall wingspan of 415 feet. At seventy percent of the half span, a stiff structural member points out in the chordwise direction and attaches to the tip of the rear wing (see Figure 5.01). The vertical distance between the front and rear wing root chords is 68 feet.

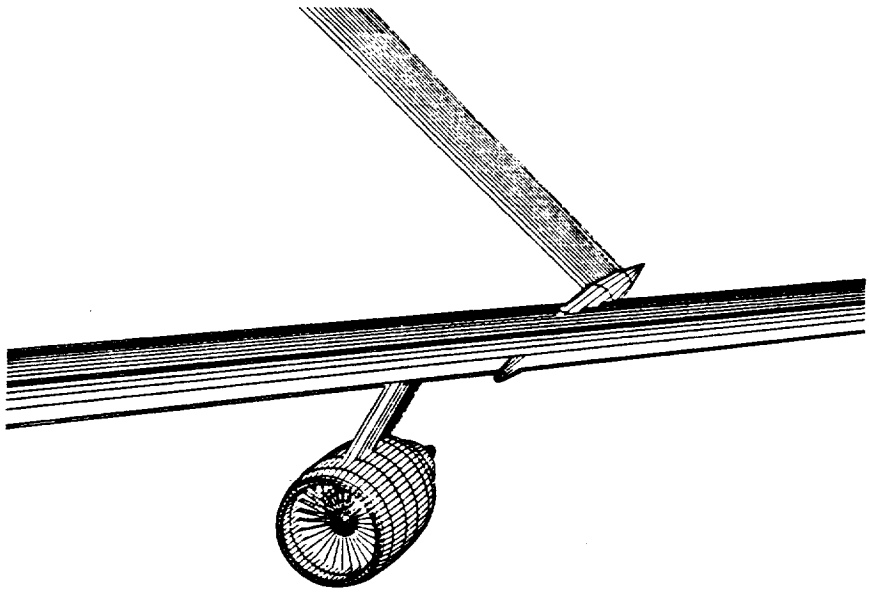

Figure 5.0.1 - Joined Wing Attachment Point

During the preliminary design of this aircraft, the aspect ratio of the wings was chosen to be 12. This number is purely a reference value calculated by dividing the entire

planform area of both wings, by the overall span. Individually however, the front and rear wings have rather high aspect ratios of 15.2 and 24.8 respectively. The idea behind our concept is that the front wing will be producing most of the lift. In order to do this, it must be of a fairly large area and aspect ratio. To avoid the large deflections and compressive loads that this type of wing would encounter, the rear wing was added as a lifting brace. Thus, the rear wing was designed with a primary role of structural brace for the front wing, and with a secondary role of lifting surface. The rear wing sits in compression, bracing the high aspect ratio front wing from large deflections during flight. Figure 5.0.2 shows a comparison of a normal cantilever wing and the *Cetaceopteryx* joined wing. On the ground, the rear wing maintains its bracing role by sitting in tension and keeping the front wing from drooping and putting dangerous compressive loads on the lower wing skin.

A NACA 63_1-412 airfoil, as shown in Figure 5.0.3, was chosen for both the front and rear wings of this aircraft. Optimization of the joined wing does in fact require that more than one airfoil be used along the span due to twisting and wing joint interference. The aerodynamic analysis involved, however, was beyond the scope of this study. With a thickness of twelve percent of the chord, this airfoil is not particularly thick compared to modern supercritical shapes. It does, however, provide sufficient volume in the front wing alone for either the primary or secondary mission fuel requirements. The front spar to rear spar distance in both wings is sixty-five percent of the chord.

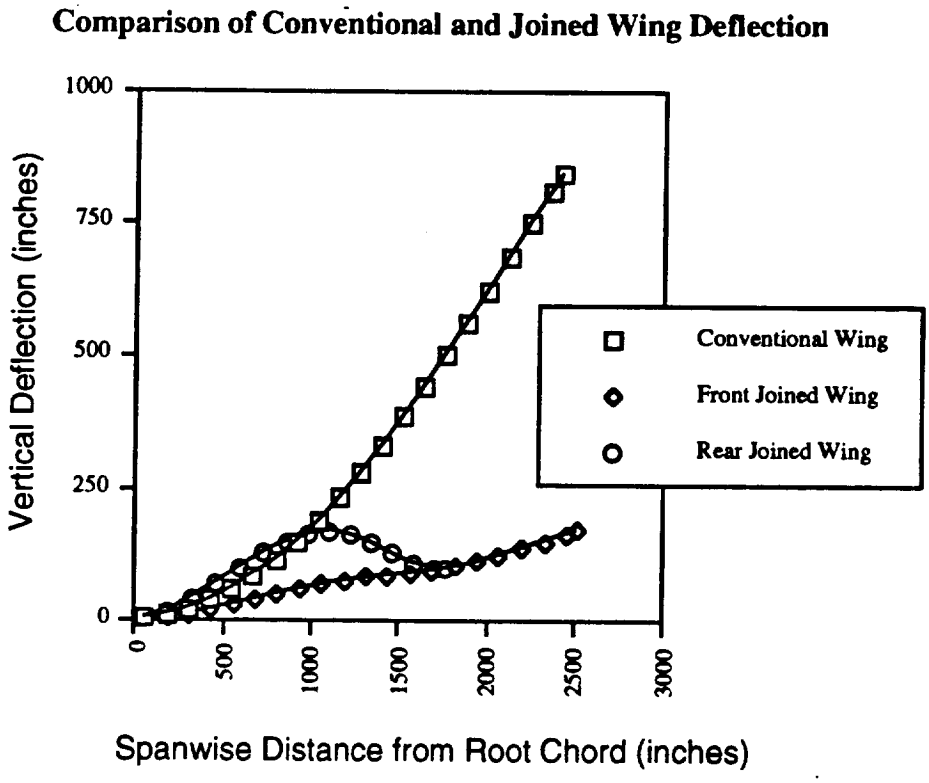

Figure 5.0.2 - Wing Comparison

The front wing holds inboard flaps from the fuselage to 55 percent of the semi span. Just ahead and above the flaps are three sets of spoilers. From 75 percent of the semi span to the tips are the ailerons. There are no leading edge or advanced high lift devices either of the wings. The rear wing however does hold elevators from 25 to 50 percent of the semi span.

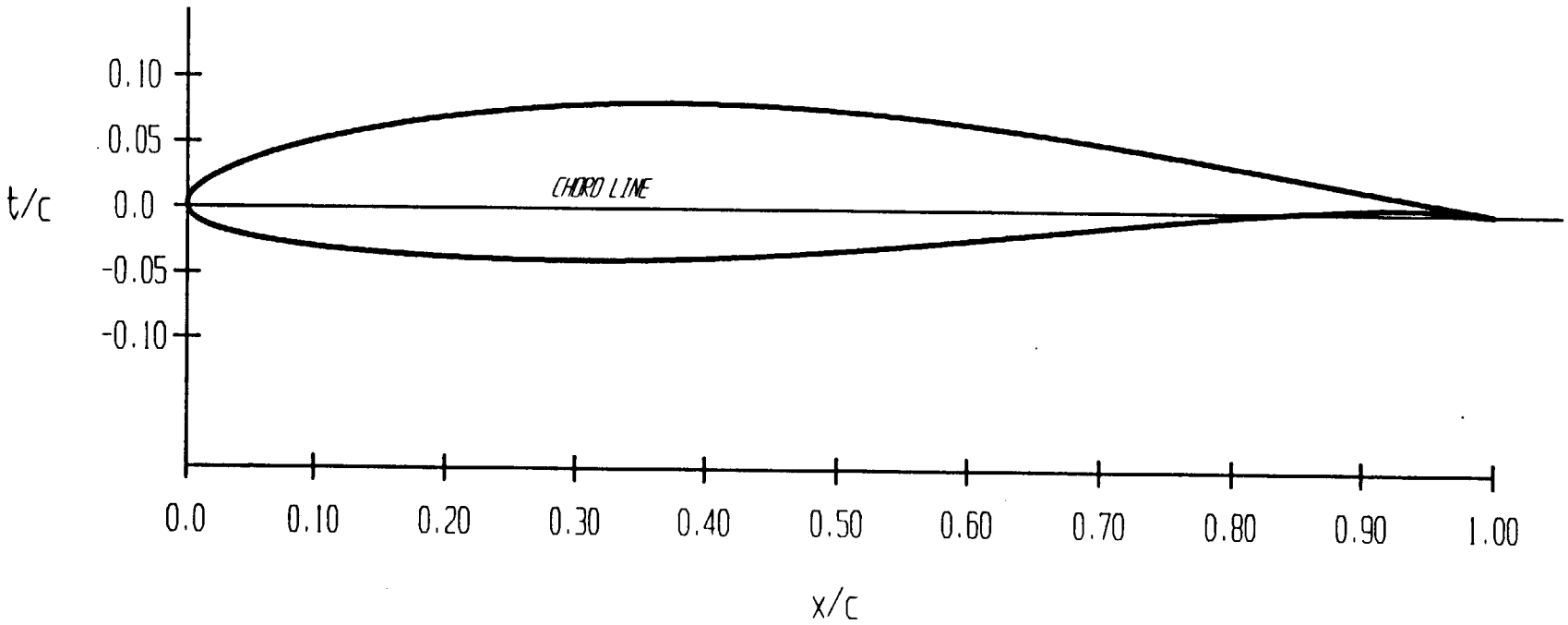

Figure 5.0.3 - NACA 63_1-412

FUSELAGE DESIGN

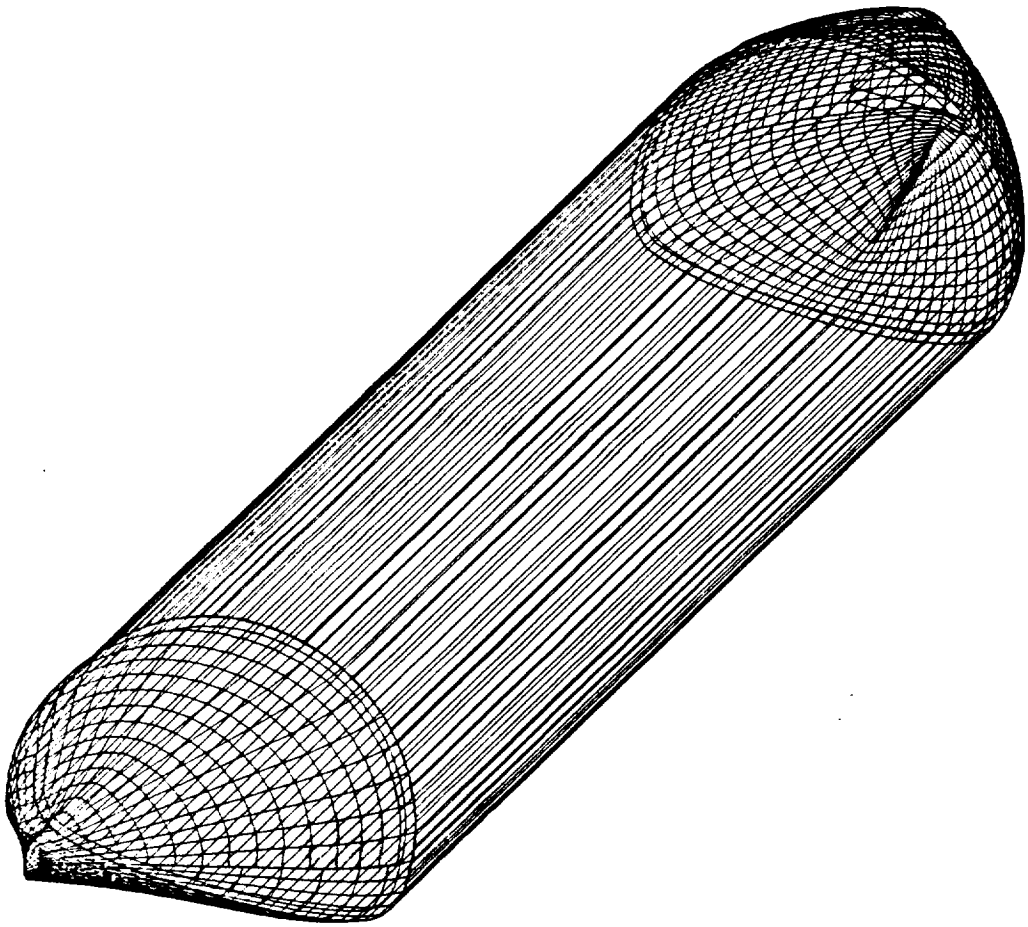

6. FUSELAGE DESIGN

The Hydra's cargo carrying capability dictated the design of its fuselage. Since the cargo floor must be relatively close to the ground in order to facilitate loading and unloading of cargo, a non-circular fuselage was necessary. If the fuselage was circular the diameter would be unnecessarily large in order to keep the cargo floor close to the ground. The non-circular fuselage is a disadvantage since the fuselage will be pressurized, however it is still the best solution. The problem will be minimized though. Since the aircraft will be used primarily for long range trips, it will not be put through excessive pressurization cycles.

6.1. Fuselage Layout

The fuselage was volumetrically sized so that it could carry six M-1 tanks, three AH-1G helicopters, twenty 463L pallets, and 200 troops as required by the RFP.[1] Placing three helicopters or two tanks across resulted in a cargo bay width of 31.5 feet. The required cargo bay length was 190 feet. Also located in the cargo bay were two loadmaster stations. One will be located at the front and the other at the rear of the cargo bay. Figure 6.1.1 shows both the cargo layout of the *Cetaceopteryx* and the *Cetaceopertyx's* ability to carry four McDonnell Douglas C-17 loads. Also shown is the fuselage cross section in Figure 6.1.2. As shown in the figure, there are two decks. The lower deck floor is only two feet from the bottom of the fuselage, thus allowing for ease of loading and unloading of cargo. The upper deck has troop seating and the cockpit which will be discussed below.

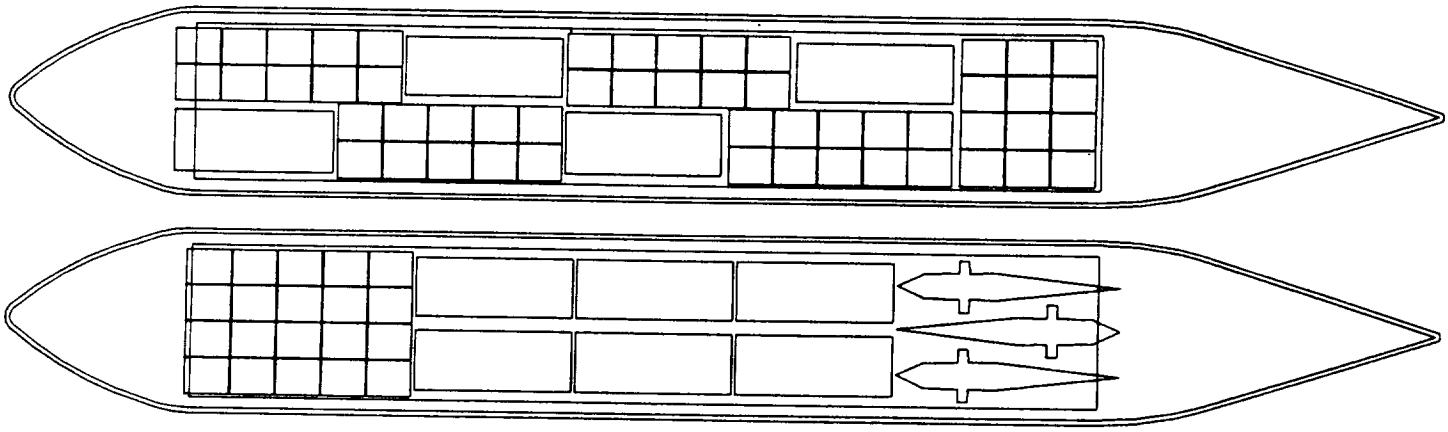

Figure 6.1.1 Cetaceopteryx Cargo Layout

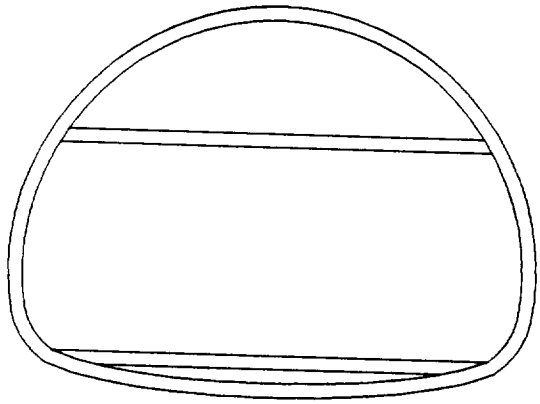

Figure 6.1.2 Fuselage Cross Section

An additional 34 feet was added to the front of the cargo bay for the aircraft's nose and 70 feet was added to the rear of the cargo bay for the aircraft's tail. This resulted in a fuselage length of 294 feet and a fineness ratio of ten.

Seating for 200 troops is located on the upper deck above the cargo bay behind the front wing box. They are seated 12 across with two aisles. The seat pitch is increased to 45 inches so that packs can be hung on the back of the seats, thereby not separating the troops from their gear. Located

with the troop seating is a self-serve galley and three lavatories. In front of the front wing box, above the cargo bay is the cockpit, a crew rest area, a self-serve galley and a lavatory. The *Cetaceopteryx* requires two pilots but the cockpit is equipped with seating for four crew members. The crew rest area has two bunks, a table and two seats. Figure 6.1.3 shows the layout of the upper deck.

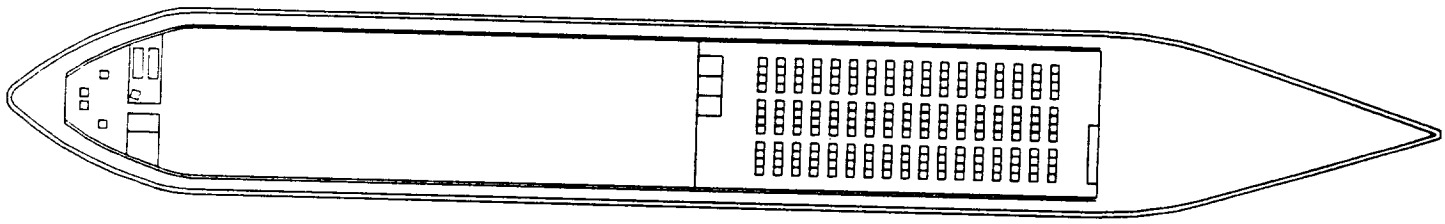

Figure 6.1.3 Upper Deck Layout

6.2. Loading and Unloading

Loading and unloading of cargo will be facilitated by having both the nose and rear of the aircraft open. The nose will hydraulically hinge up similar to the Lockheed C-5. A ramp can then be pulled out from under the cargo floor. The rear will open by lowering the underside of the tail which will then serve as the ramp similar to the McDonnell Douglas C-17. The cargo floor is five feet from the ground and the ramp angles are each eight degrees.

The troops and air crew will also enter the aircraft through either the front or rear ramp. They will then climb stairs to reach the upper deck. For emergency purposes the aircraft has six doors equipped with inflatable slides. Two are located on the lower deck and four on the upper deck.

PROPULSION

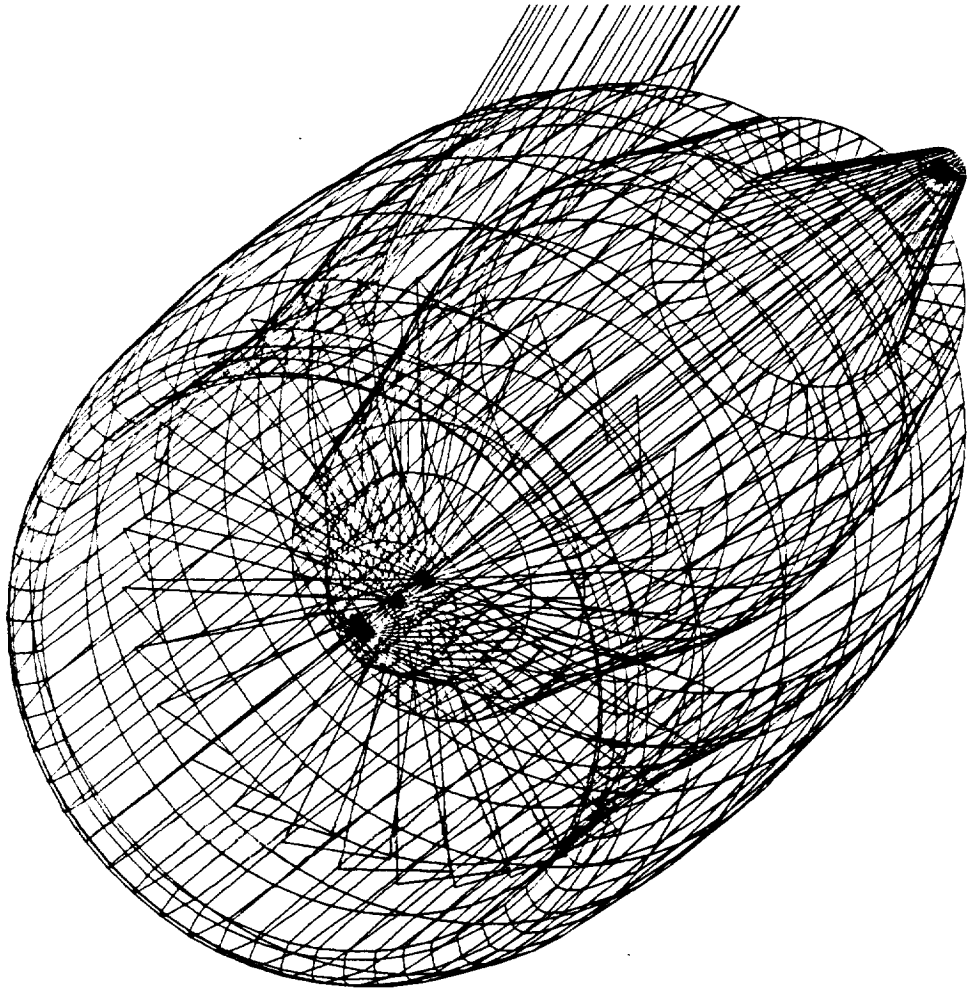

7. PROPULSION SYSTEM

NOTE : The Cetaceopteryx's *propulsion system design is based on proprietary information provided by the General Electric Company. Consequently, detailed data and calculations can not be furnished.*

One of the key elements of any aircraft design is the propulsion system; this is especially critical for a military cargo aircraft the size of *Cetaceopteryx*. The key challenges it faces are providing sufficient thrust for take off while maintaining low specific fuel consumption for efficient operation during cruise. To meet these demands, Hydra has chosen the GE90 high bypass turbofan as the most suitable power plant for the *Cetaceopteryx*.

7.1. Considerations

The propulsion system selection to be installed on *Cetaceopteryx* focused on several major concerns: high performance, fuel efficiency, available thrust, foreign object damage, maintenance, and the ever increasing environmental concerns for noise and emission pollution. Due to the unconventional configuration of *Cetaceopteryx*, the engine location was dependent on factors such as the structure of the aircraft and interference drag. There were three possible engine mounting locations : the fuselage , front wing, and rear wing. Fuselage installation was decided against since it would move the aircraft center of

gravity aft which in turn would affect aircraft stability. Since the rear wing has an anhedral of 20.8° and its vertical position with respect to the ground varies from 90 ft at the root of the wing to 31 ft at the joint location, installation on the rear wing would have caused extreme maintenance problems as well as creating an excessive pitching down moment, an undesirable behavior during take-off. With that, the engine location was constrained to installation below the front wing. With this placement the ground clearance ranges from 10 to 17 ft. Although this placement causes some maintenance difficulties, it is the most suitable location. Figure 7.1.1 shows the engine placement on the front wing.

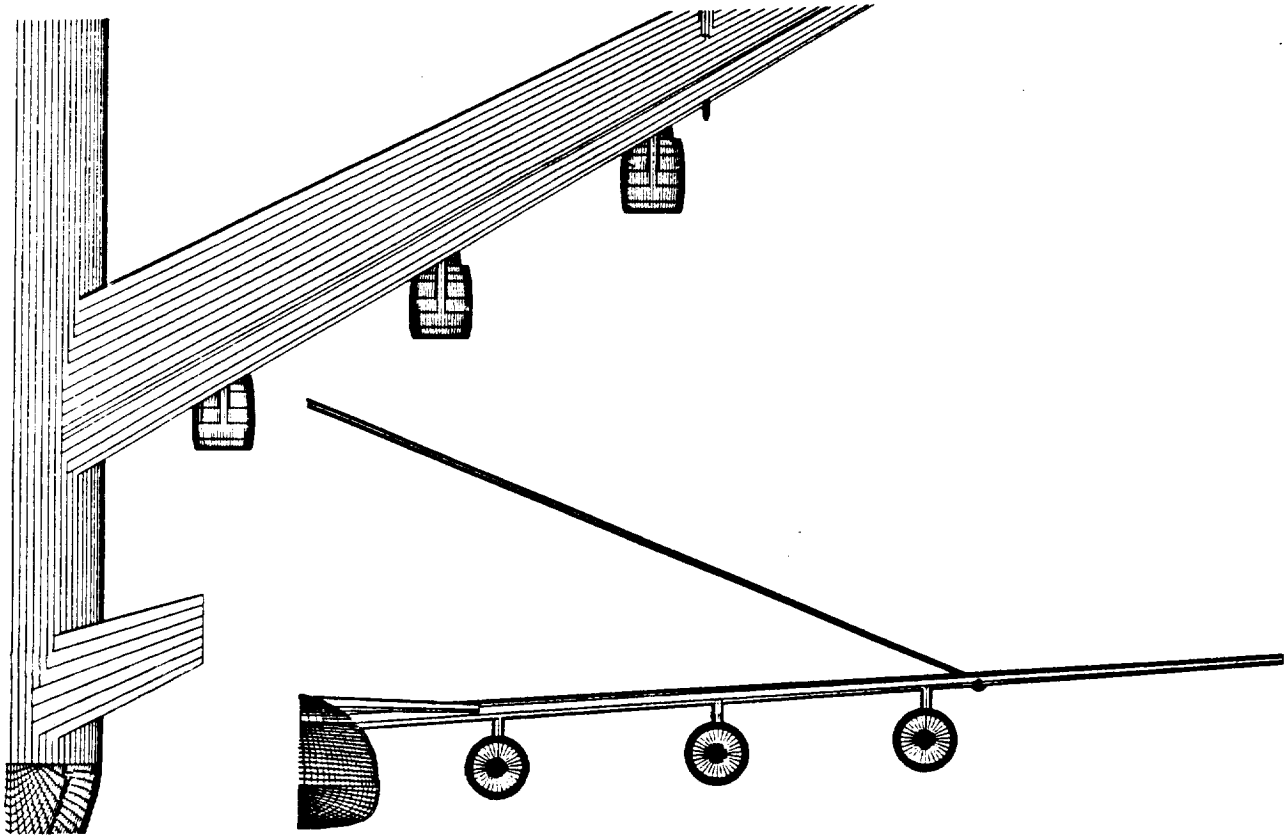

Figure 7.1.1 - Engine Placement

7.2. Thrust Requirements

From the preliminary sizing, with 164 wing loading (W/S) and thrust to weight ratio (T/W) of 0.29, the required thrust for *Cetaceopteryx* was 620,600 lbs. In order to meet this thrust requirements as well as minimize the number of engines, the aircraft needed efficient engines which would also satisfy the high thrust demands. Different types of engines were explored for the aircraft's propulsive system. The two candidates were turboprop and turbofan engines. Due to the low available thrust inherent in the turboprop engines currently in production, this option was discarded since an excessive number of engines would be required. Therefore, turbofan engines were found to be the best alternative. With advancements in technology and increasing growth in composite material developments, today's turbofan engines could provide sufficient thrust to satisfy the aircraft's take-off and one engine inoperative requirements.

A number of existing turbofan engines were considered. In order to minimize the number of engines, development of a new engine which would satisfy our propulsion needs seems to be the most practical solution. However, by using an existing engine, the extra cost of developing one may be deferred. The most promising candidates were Pratt & Whitney P&W 4084 with 84,000 lb of thrust and General Electric GE90 with 105,000 lb of thrust. Thus, the most efficient engine which would satisfy *Cetaceopteryx's* thrust requirements as well as fuel efficiency, noise, and emission demands was the GE90 high bypass turbofan engine. It was determined that six engines were needed to meet *Cetaceopteryx's* required 620,600 lb of total thrust, with allowances made for electrical, mechanical, and pneumatic

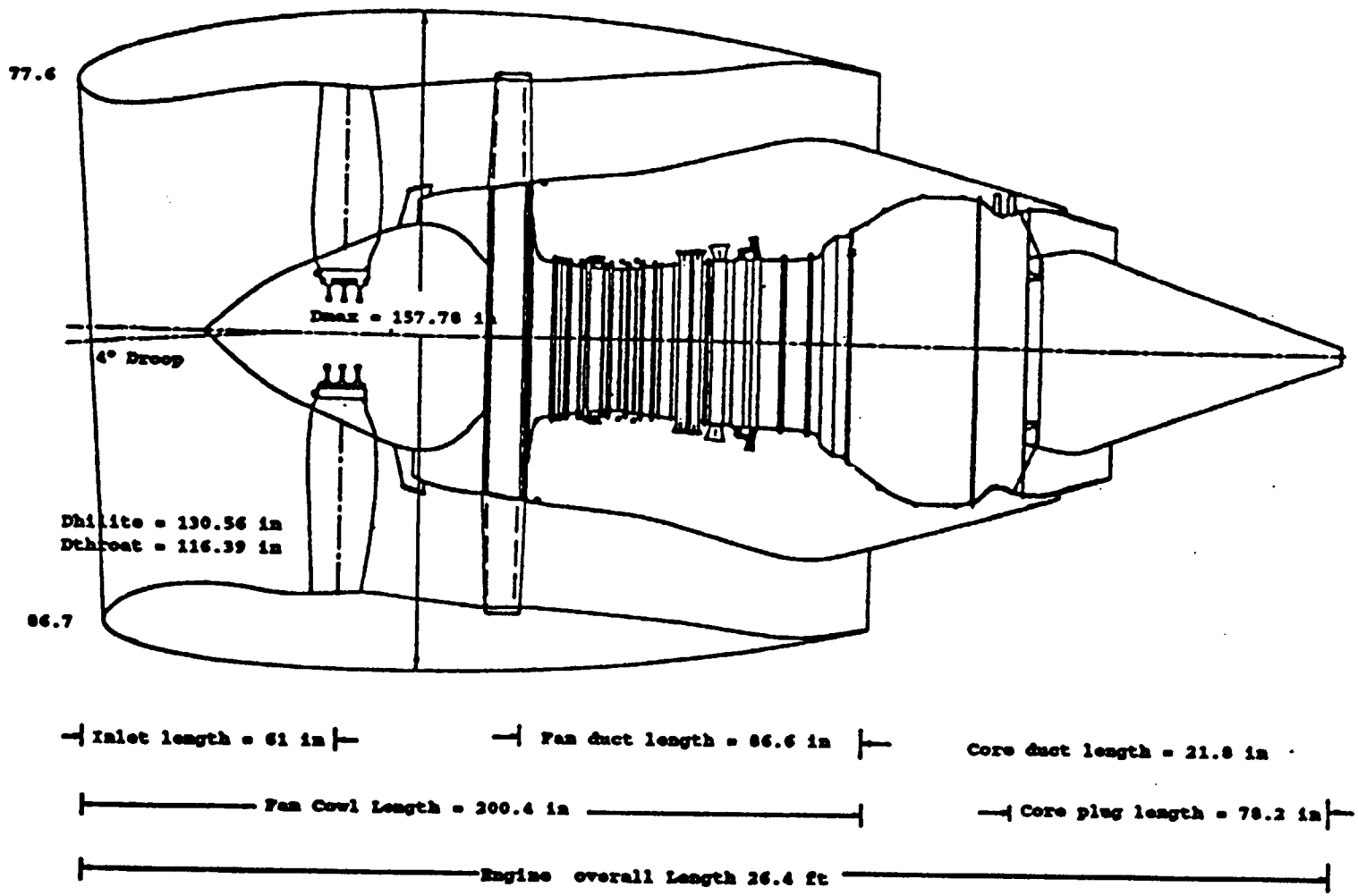

Figure 7.2.1 GE90 Engine Dimensions

power extraction during take-off (2696 lb), climb (2249 lb), and cruise (2052 lb).

7.3. Engine Characteristics

The GE90 key dimensions are shown in Figure 7.2.1. As can be seen from 26.4 ft overall length, 10.3 ft fan diameter, and 13.1 maximum diameter, GE90 is the largest engine under development. Compared with Pratt & Whitney 4168 (68,000 lb thrust, 13.5 ft length, 8.7 ft diameter, 14,000 lb complete system weight), the GE90 is 96% longer, 51% wider, 50% heavier, and produces 54% more thrust for a 44% increase in thrust to weight ratio.

The GE90 features an increased bypass ratio from the 5:1 typical of today's engines to 9:1, the highest bypass ratio of any ducted fan engine in production. The compressor pressure ratio is 23:1 and the overall pressure ratio exceeds 45:1. This combination of increased bypass and pressure ratios reduces specific fuel consumption by more than 9% compared to conventional high bypass turbofan engines due to its thermodynamic cycle. This is shown in Figure 7.3.1. In addition, this improvement in performance, significantly reduced emissions and noise signatures.[11]

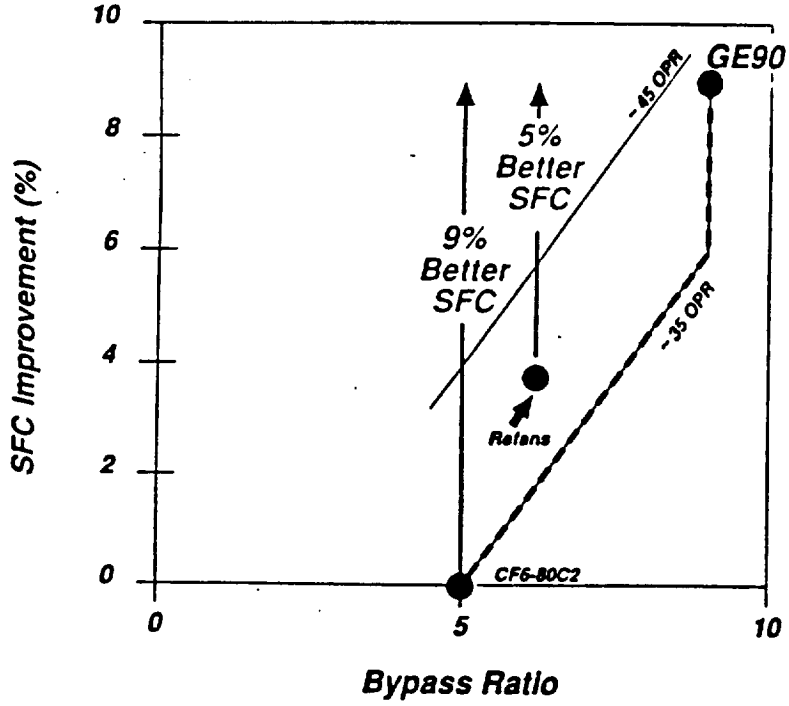

Figure 7.3.1 - GE-90 Cruise SFC Cycle Comparison

The design of GE90 permits easy transportation since the modular design allows the fan stator case to remain with the aircraft, reducing spares investment and simplifying transportation requirements. The split engine can be transported on widebody freighters, while the spare propulsion can be carried on all freighters. GE90 can be disassembled into major modules for transport in the lower lobe of widebody passenger aircraft.[11]

The GE90 dual-dome combustor's staged burning provides significantly reduced emissions, improved operability and reduced engine length; all without penalty to specific fuel consumption. Compared to current large turbofans, the combustor reduces nitrogen oxide (NO_X) emissions by more than 34%, presented in Figure 7.3.3, carbon monoxide (CO) emissions by over 25%, and unburned hydrocarbon (HC) emissions by more than 60%.[12]

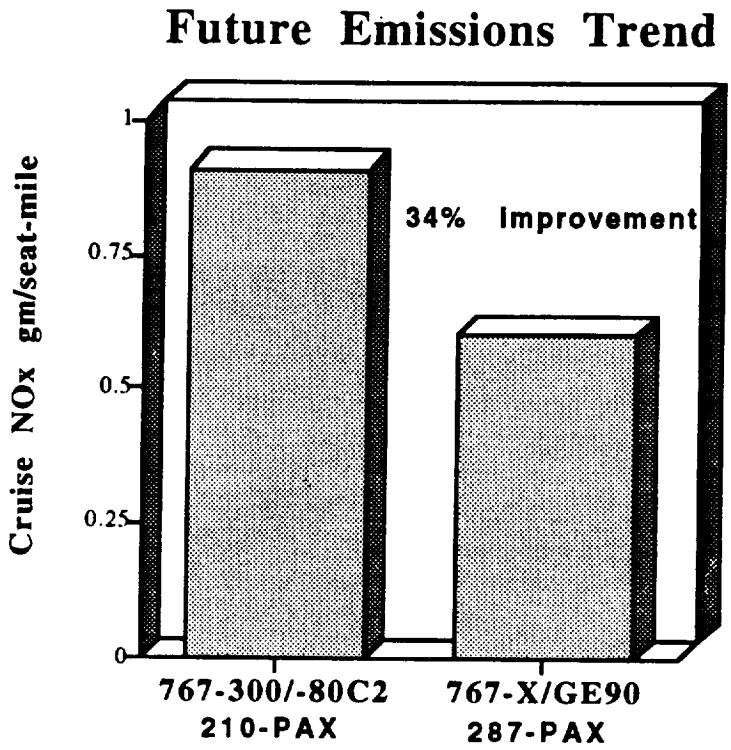

Figure 7.3.3 - Emissions

Because of its higher bypass ratio, along with its lower fan tip speed, fan pressure ratio, and exhaust velocity, the GE90 produces less noise than other turbofans in its class. Since this design optimally integrates acoustic objectives with other engine requirements, the aircraft will be able to operate efficiently into and out of the most noise sensitive airports.[12] Although there are no noise or emission restrictions for military aircraft's, the environmentally conscious Hydra design team chose to implement a "green" philosophy in the design of *Cetaceopteryx's* propulsion system.

7.4. Inlet Design

Since the GE90 is being tested and refined for the Boeing 777, and it is the objective of this design team to reduce further developmental costs to the maximum extent possible, the inlet design selected is similar to that of the Boeing 777, a conventional circular inlet configuration suitable for *Cetaceopteryx's* subsonic flight regime. Given the aircraft's cruise condition, the required inlet area was determined to be 10639 in^2, with a nacelle incidence angle (droop) of 4° to compensate for variations in the aircraft's angle of attack as shown in Figure 7.4.1. These variations in angle of attack, which change the angle of the airflow with respect to the centerline of the engine, typically occur during take-off rotation and landing phases of flight and range from 1.2 Vstall to 1.6 Vstall. Figure 7.4.2 shows this variation in angle of attack.

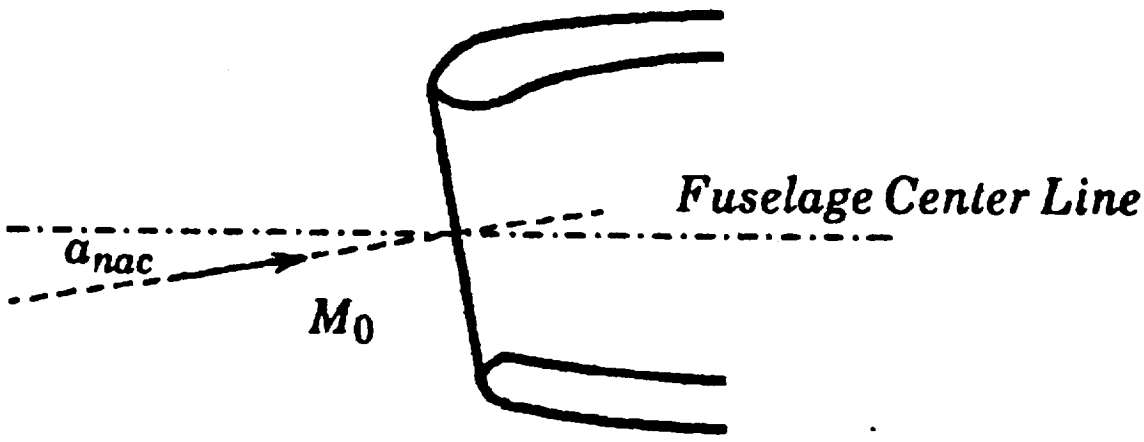

Figure 7.4.1 - Incidence of the Nacelle Face for GE90

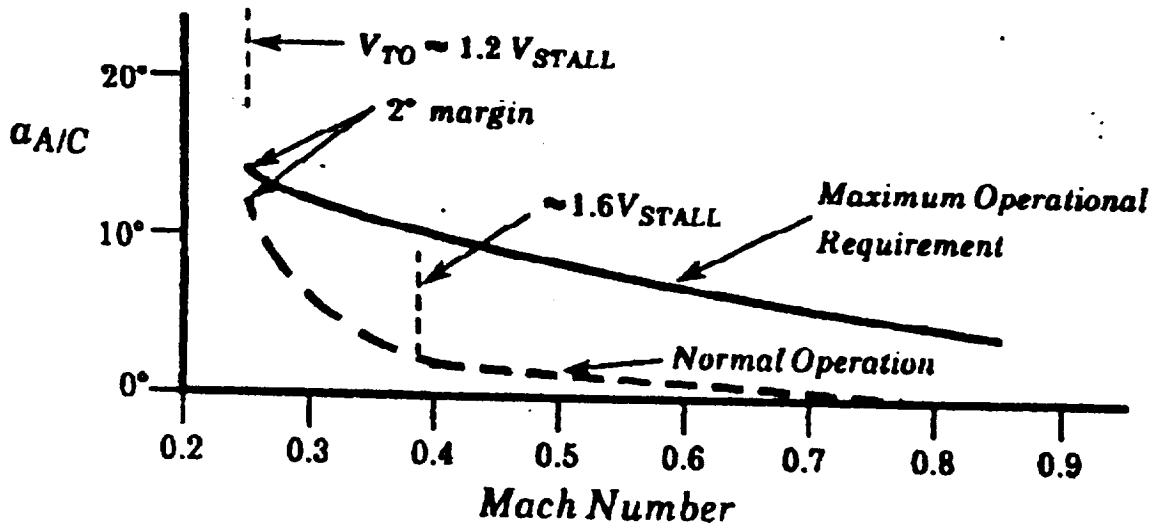

Figure 7.4.2 - Variation in Angle of Attack

7.5. Engine Performance

Due to proprietary nature of the information provided by General Electric, graphs and data for this section have been omitted from this report.

LANDING GEAR

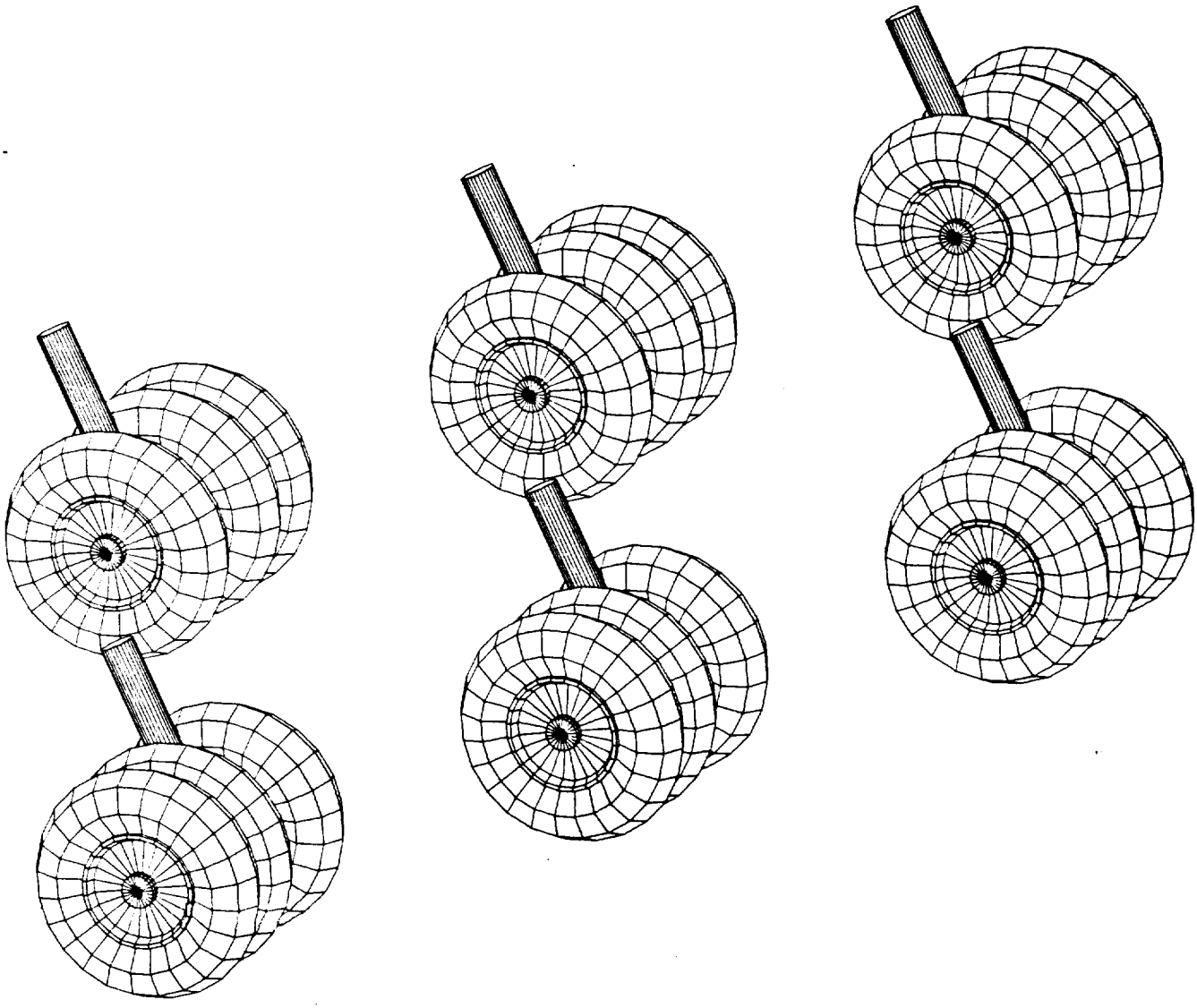

8. LANDING GEAR DESIGN

8.1. General

In accordance with the design methods described by References 9 and 10 (Roskam and Currey), the *Cetaceopteryx's* landing gear consists of nose and main gear arranged in a semi-conventional configuration (Figure 8.1.1). One of the overriding considerations in the design of the aircraft's landing gear system was the need to keep the weight and size of the gear as low as possible while still retaining the capability of being able to function under the tremendous loads imposed on it in normal operations.

The resulting landing gear characteristics are summarized in Table 8.1.1 as follows:

Table 8.1.1 Landing Gear Characteristics

Static Nose Gear Load (% WTO)	13.0
Static Main Gear Load (% WTO)	92.0
Maximum ACN	110
Turn Radius (feet)	170
Max Nose Gear Steering Angle	60°
Max Main Gear Steering Angle	20°
Max Allowable Rotation Angle	15°

At first glance, the ACN rating of the aircraft might appear to be extremely high. However, it is anticipated that the aircraft's home base/initial airfield -- the point that it will be heaviest -- will be a specially prepared facility with runways with the necessary reinforcement to handle the

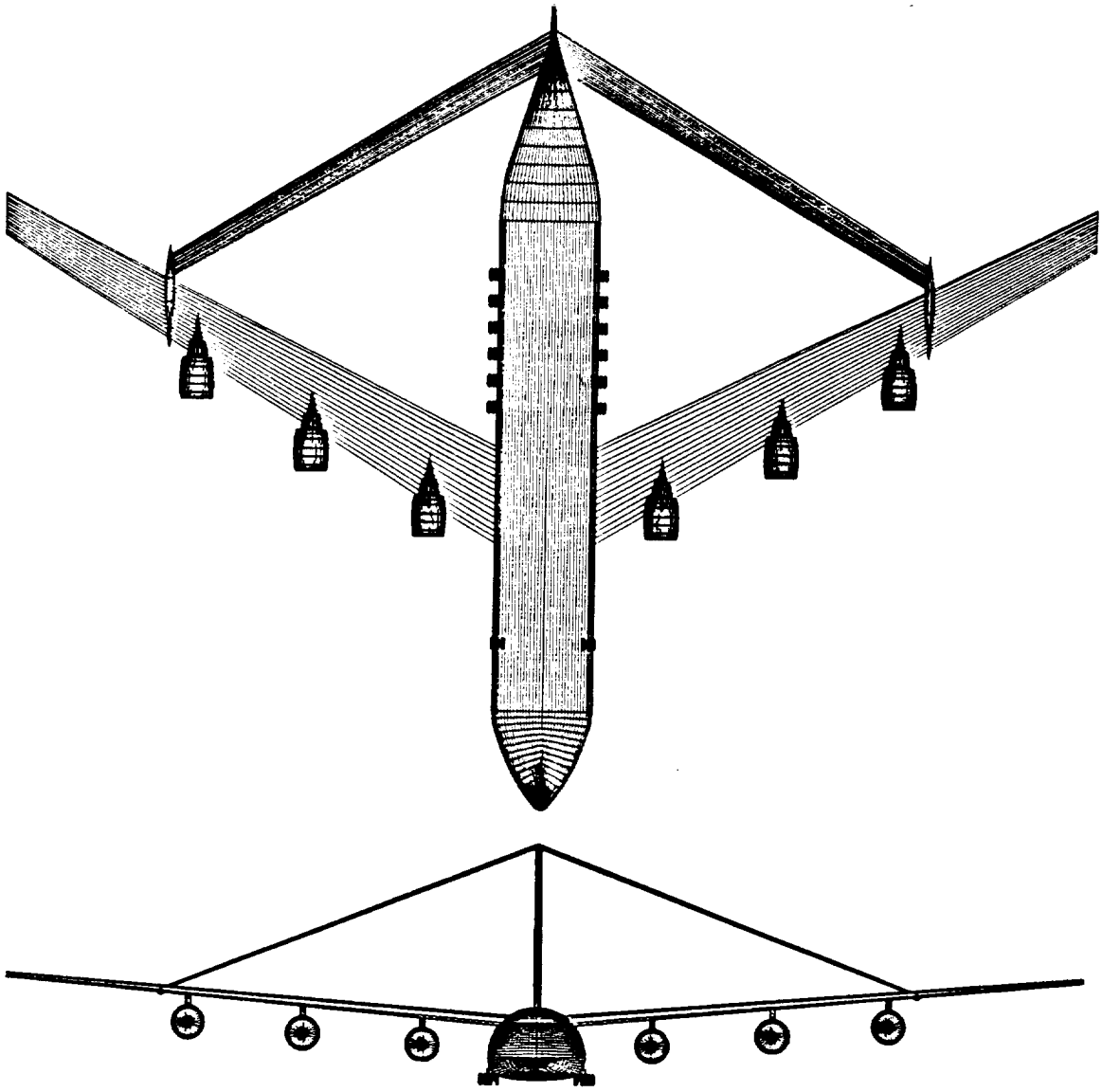

Figure 8.1.1 - Landing Gear

loads imposed by *Cetaceopteryx*. During normal operations, however, the aircraft's weight has reduced to acceptable levels by the time it has reached the intermediate airfield, where its ACN has fallen to 87. Even if the intermediate point runway surfaces are not sufficiently hardened to withstand long-term use, it is not anticipated that the *Cetaceopteryx* will be operating from a runway for an extended period of time or that, in time of war, runway errosion will be of prime importance.

As a result of the design philosophy mentioned above, tires with the highest possible load-carrying capability were selected as the basis for the gear design in order to

distribute the load through as few wheels, tires, and struts as possible, maintaining system simplicity and reducing failure probabilities. The wheel/tire combination chosen was the B. F. Goodrich 56x16 Type VII (high pressure) tire, the characteristics of which are tabulated below in Table 8.1.2.

Table 8.1.2 Tire Characteristics

Diameter (inches)	56
Width (inches)	16
Max. Load (pounds)	76,000
Max Inflation Pressure (psi)	315

8.2. Unique Features

Several unique features distinguish the *Cetaceopteryx's* landing gear from that of other large transport aircraft, the most important of which is main gear steering. In the past, deflection of the main gear's wheel rotation axis has been limited to the Boeing B-52 Stratofortress bomber and Lockheed C-5 Galaxy transport, where the capability was used to correct for crosswind landing situations. In the case of the *Cetaceopteryx*, however, the ability to deflect the main gear 20 degrees left and right of centerline is used for ground steering in order to reduce the turning radius (Figure 8.2.1). While this feature could also be used for crosswind landing correction, the ability of the joined wing to create direct sideforce – for it to counteract a crosswind without crabbing – reduces its importance in this role.

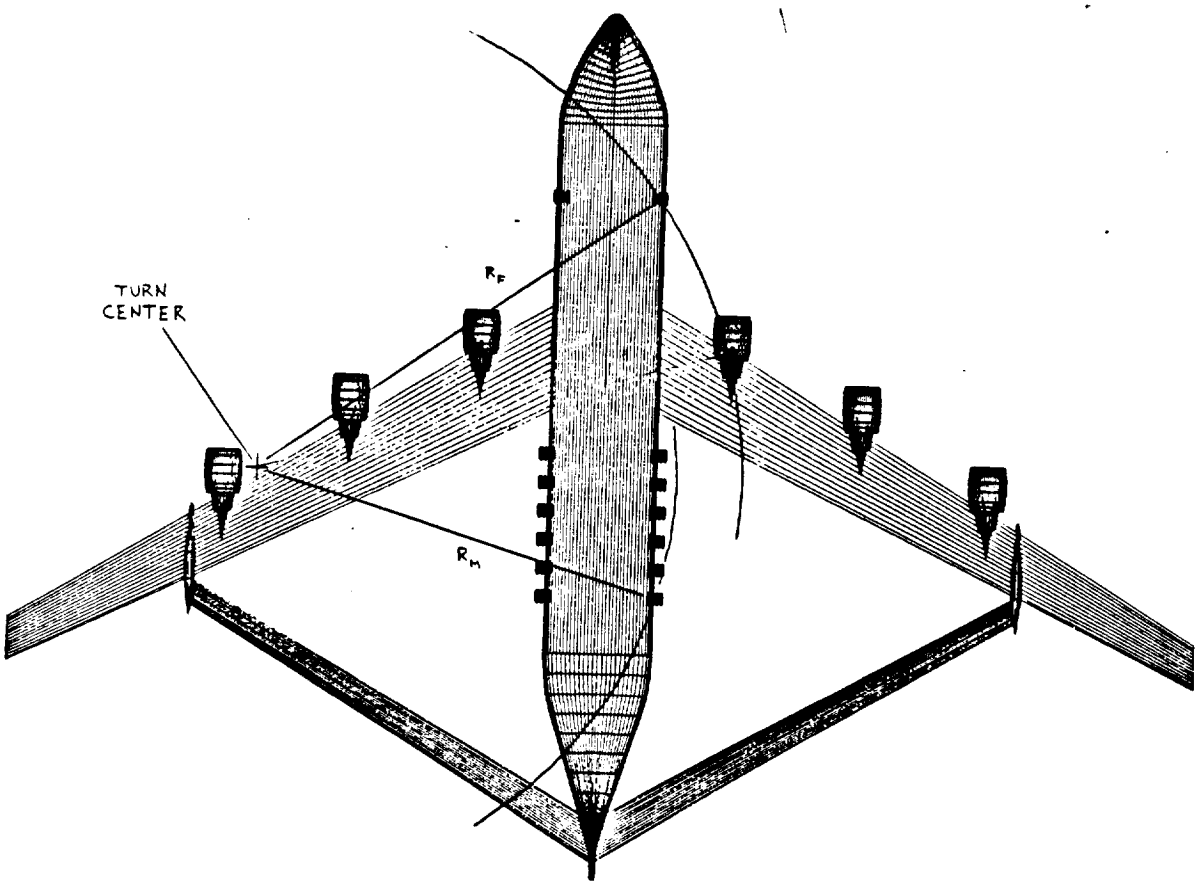

Figure 8.2.1 - Turning Radius

In addition, the *Cetaceopteryx* is capable of in-flight tire pressure adjustment, a feature seen previously in the Lockheed C-5. The Galaxy adjusts its tire pressure for optimum flotation when operating on unsurfaced airfields, a role the *Cetaceopteryx* is not intended to perform. Instead, the pressure adjustment system of the *Cetaceopteryx* is intended to minimize stresses on paved airfields, many of which, at the intermediate point in particular, may not be of sufficient strength to withstand repeated operations by an aircraft weighing 1.6 million pounds (based on primary mission landing weight). In addition, since the aircraft weight varies between 2.14 million pounds at takeoff and 750,000 pounds at landing, the runway stresses imposed by the aircraft vary radically during the span of one mission. In-flight tire pressure

control, therefore, is deemed a worthwhile complication in the design.

8.3. Main Gear

The main gear consists of 36 wheels arranged in two rows of six struts, with three wheels per strut. Each triple bogie consists of a corotating pair of wheels outboard of the strut and a single wheel inboard in order to facilitate wheel removal, replacement, and maintenance. The track is 45 feet, which is fairly narrow for an aircraft the size of *Cetaceopteryx*; however, this track is dictated by the facts that the fuselage is itself comparatively narrow compared to the wingspan and that there are few other suitable mounting locations.

During retraction, the gear rotates 90 degrees in the same manner as the main gear of the McDonnell Douglas C-17 in order to reduce to a minimum the cross-sectional area presented to the free-stream by the gear and the streamlined gear fairings (pods).

In the event of the failure of a main gear tire at maximum gross weight, the remaining tires are capable of supporting the redistributed load. At operational empty weight, it is possible to hydraulically lift any bogie clear of the ground for maintenance without overloading the remainder of the gear.

8.4. Nose Gear

The nose gear consists of six wheels arranged in two triple bogies in much the same manner as the Lockheed C-5 nose gear. In *Cetaceopteryx's* case, though, the two nose gear struts are located much further apart (at the edges of the

fuselage) due to lack of retraction space beneath the cargo bay. The nose gear track is 40 feet, which, because it is not significantly smaller than the track of the main gear, tends to cause the overall gear configuration to resemble a tandem gear. However, because the main track is larger than the nose gear's, a case could also be made for calling it a conventional arrangement.

In any case, because the nose gear shares identical wheel size, bogie configuration, and retraction sequence as the main gear, it is also capable of sustaining the same failure load cases. However, the nose gear will be overloaded in the event of on- or off-loading the heaviest of the possible cargo (M-1 Main Battle Tank). To rectify this problem, a pair of hydraulically extended braces are provided that deploy during cargo handling in order to reduce the loads transmitted to the nose gear.

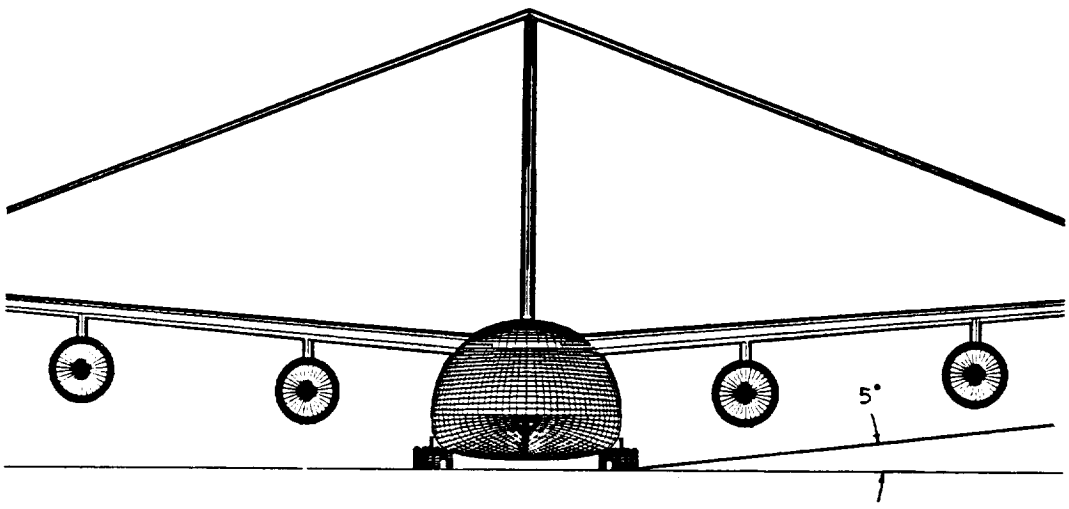

Figure 8.5.1 - Tip-Over Criteria

STRUCTURES

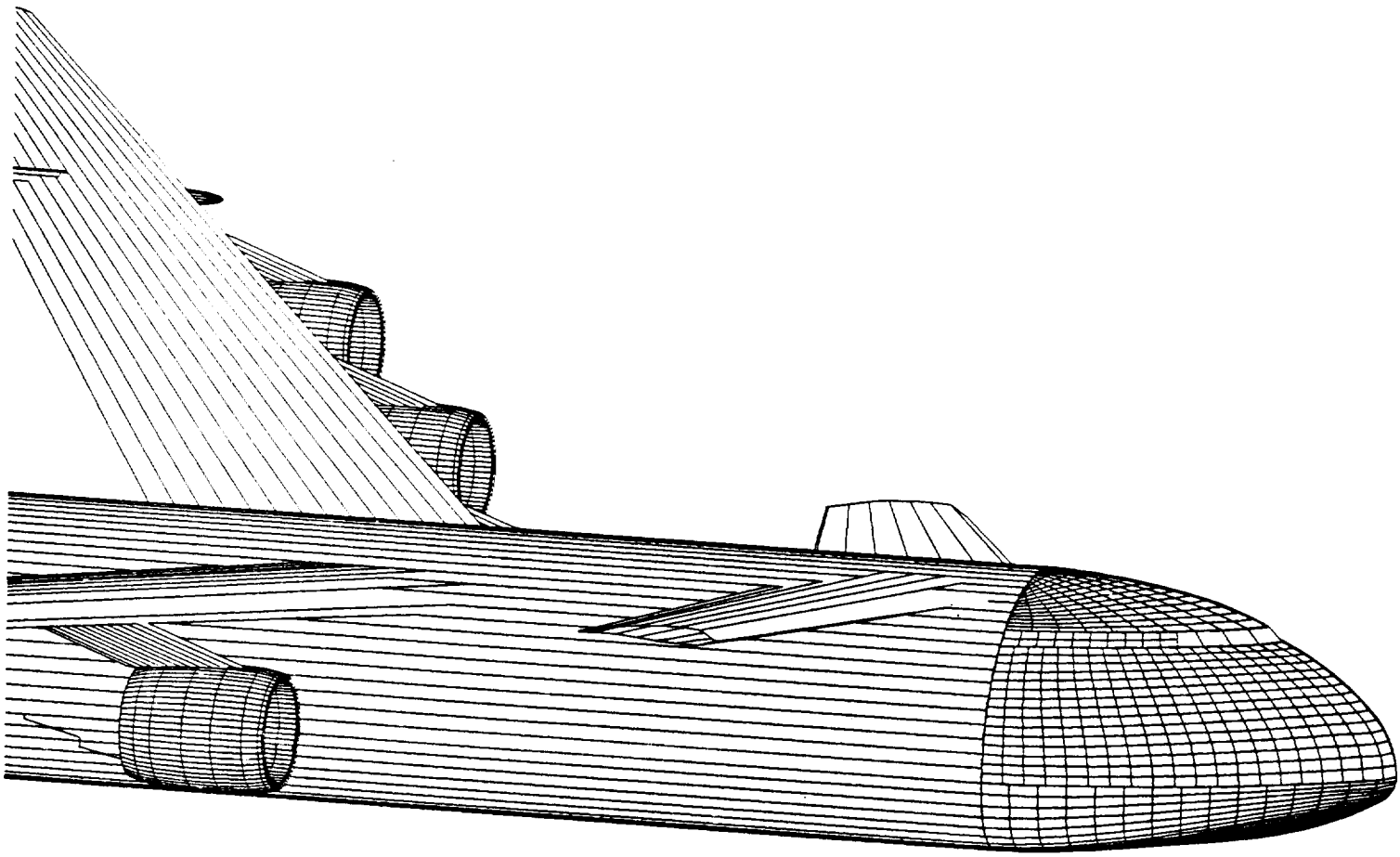

9. STRUCTURES

The structural configuration of the Cetaceopteryx was one of the most unique and challenging problems encountered in the aircraft's overall design. The size of the aircraft, the decision to use mostly composite material, and the joined wing configuration itself , were the main contributors to the complexity of the structural analysis. The complexity of the design does not however detract from the fact that the Cetaceopteryx is a lighter, stronger, aerodynamically superior aircraft.

9.1. V-n Diagram

The V-n diagram is shown in Figure 9.1.1. As can be seen from the diagram, the *Cetaceopteryx* is not a gust sensitive aircraft, and can be operated at normal cruise speed in turbulence conditions. It has the ability to maneuver at a load factor of 2.5 g's, but in the early phases of the mission, it can only do so at altitudes of no higher than 26,000 ft. In figure 9.1.2 a V-n diagram shows the gust and maneuver sensitivity of the *Cetaceopteryx* if it was to fly at an altitude of 35,000 ft. It can be seen that here, the aircraft is very gust and maneuver sensitive and shows why the *Cetaceopteryx* must fly at a lower altitude. Yet, it can maneuver at a load factor of 2.5 g's and at altitudes greater than 26,000 on the return trips, when it is much lighter. The *Cetaceopteryx* had a cruising speed of 306 KEAS, and a dive speed of 382 KEAS under high wing loading. It will stall at a speed of 191 KEAS.

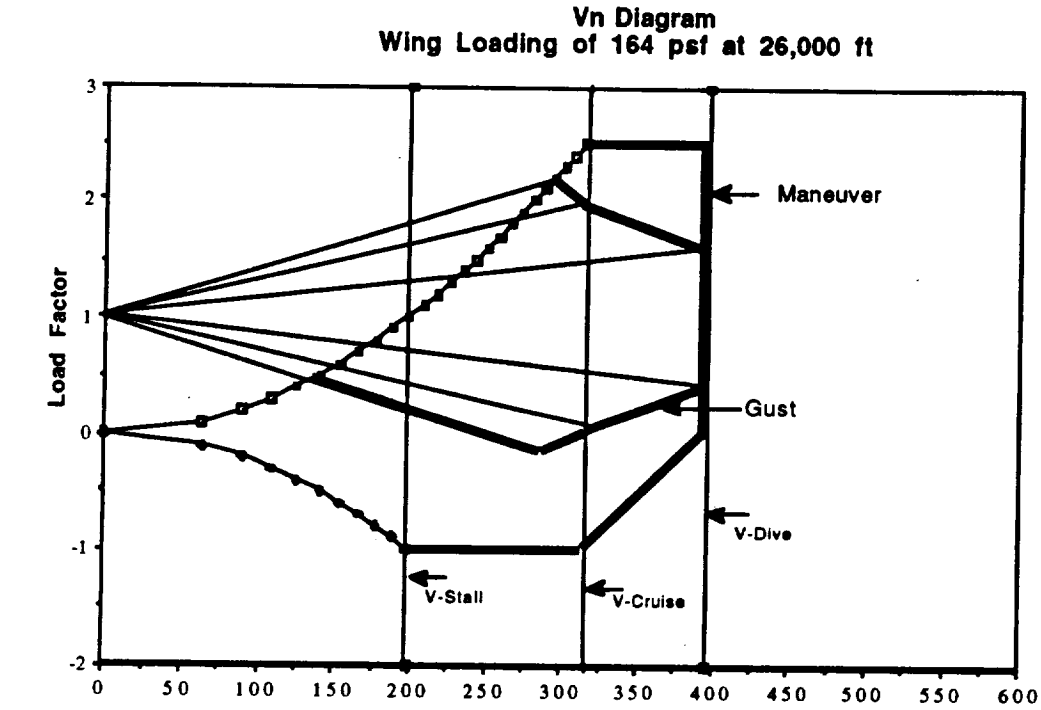

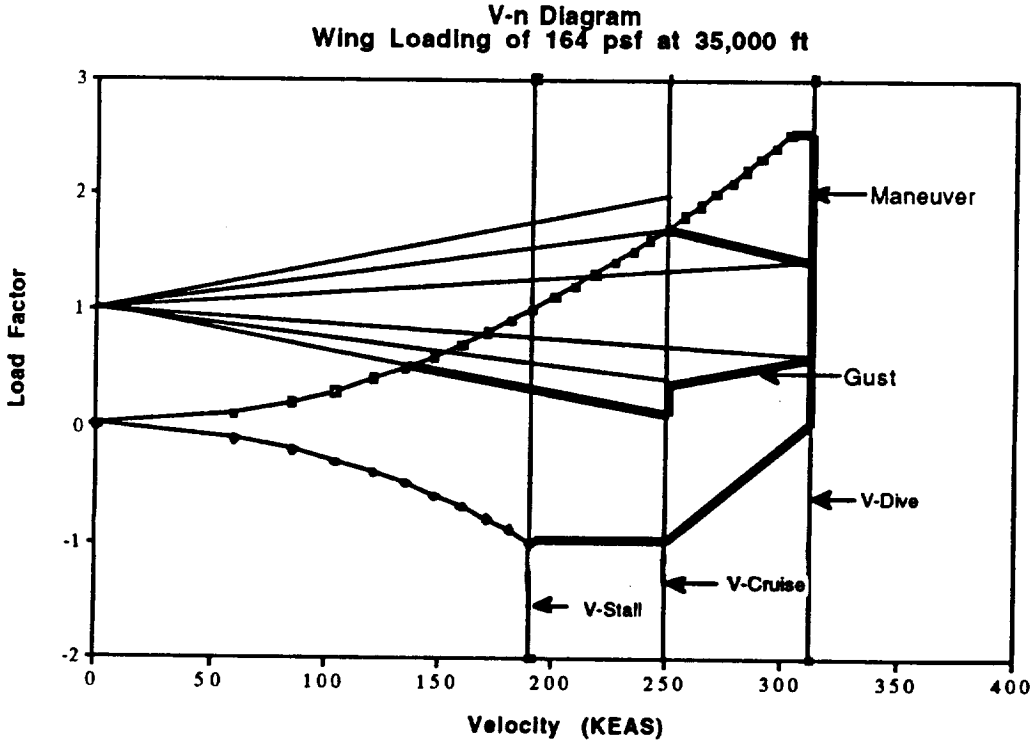

Figures 9.1.1 and 9.1.2 - V-n Diagrams

9.2. Materials

The material used most widely in this aircraft is graphite-epoxy composite (Gr-Ep). Graphite Epoxy is a polymer matrix composite that has been the mainstay composite material in the defense industry for the past 25 tears. The main advantages of this material over other composites are that it maintains the best combination of strength, stiffness, information base, and cost. Graphite Epoxy was used for almost all structural members and for the outer skins.

There are three main areas where, for various reasons, composites were not used. The first area is the vertical tail, where large bending loads from the rear wing constituted a problem. The rear wing attaches to the tail at a point approximately 60 feet above the top of the fuselage. If one side of the wing should stall and lose its lift, or if uneven loading occurs along the wings, a large side force would be applied to the tail. For a stiff tail made of composites, these side forces would transmit large twisting moments in the fuselage. In order to eliminate the extra structure required to reinforce the fuselage, the tail spars were designed for a soft 2024 aluminum that would absorb much of the force by flexing.

The landing gear was designed for steel, much like conventional landing gear in current aircraft. Steel was chosen because it is strong enough to handle the enormous compressive stresses involved in landing.

Standard materials were also used in the engine nacelles, where temperatures are higher than 300°F rated Graphite

Epoxy can handle. Third party nacelles could be used to cut costs.

9.3. Wing Design

Due to the *Cetaceopteryx's* joined wing configuration, the wing structural design significantly differs from the conventional design usually found in commercial and military transports. Firstly, the rear wing structurally braces the front wing, increasing structural stiffness. Secondly, the bending axis of the wings is along the line between the front wing root to the rear wing root, and not in the horizontal plane as with conventional cantilever wings. This makes an asymmetric wing box (see figure 9.3.1) the optimal structure for this type of wing, because it maximizes the box's moment of inertia by placing as much spar material as far away from the bending axis as possible. This makes the wing box more structurally efficient for the amount of material used, reducing the weight of the wing box.

Figure 9.3.1 An Asymmetric Wing Box

Thirdly, the asymmetric wing box design makes it desirable to make the spars farther apart than in a normal wing design. This allows more fuel volume in the wing, which will help relieve the wing loading.

9.4. Structural Analysis of the Joined Wing

The Hydra team used the Joined Wing Structural Analysis and Optimization program, or JWOPT32, a joined wing analysis program created by John Gallman.

JWOPT consists of several specialized subroutines which work together in an iterate manner to structurally optimize the joined wing, minimizing weight and drag. Jwopt starts with an input file that describes the aircraft in terms of overall weight, basic dimensions, drag polars, and airfoil shape. It then uses that input data to create clearly defined front and rear wings in three dimensions.

Once the geometry is defined, and the airfoil coordinates are known, JWOPT determines the optimum linear twist along the semispan for minimum drag by solving the Prandtl-Glauert equation for inviscid, irrotational, subsonic flow :

$$(1+M_\infty^2)U_x + V_y + W_z = 0$$

where U, V, and W are the components of flow in the x, y, and z directions. This particular subroutine in JWOPT is actually the code for LinAir, an incompressible flow analysis program. LinAir solves Prandtl-Glauert by superposition of discrete line vortices. Once the circulation strengths across the wings are determined, the Kutta-Joukowski relation,

$$\boldsymbol{F} = \rho \boldsymbol{V} \times \boldsymbol{\Gamma}$$

is used to find the lifting force and moment contribution from each panel along the wings. This subroutine therefore determines the aerodynamic loads on the wings.

Once the aerodynamic loads have been determined from the above subroutine, JWOPT begins to optimize the structure. This subroutine treats the wings as inextensible beams divided into a finite number of sections with known inertial properties. It then finds the deflections and rotations due to local forces and moments that result from the applied aerodynamic loads, the beam weight, and unit reaction forces. Next, superposition and unit load analysis were used to find the joint reactions. At this point all information needed to analyze the wing box is known except for the optimal cross sectional area and thus the moments of inertia. The input file has data on the user specified maximum and minimum skin thicknesses and cross sectional areas. Once the forces are known at all of the spanwise locations on the wing, the cross sectional area is simply sized so that the maximum allowable material stress at that location is not exceeded. JWOPT then integrates along the wingspan element areas to determine the total beam volume. Knowing the material density from the input file, the total beam weight may then be calculated. The weight from this calculation is compared to the weight of the original un-modified beams. If the weights are within a user specified tolerance then the program ends with that data. If however the weights are outside the tolerance then the program begins the analysis again using the modified cross section distribution calculated in previous iteration.

For the Cetaceopteryx configuration, JWOPT came up with the following root chord values:

	Shear(lbs/in^2)	Moment (in.lbs)
Front Wing:	1.01×10^6	4.90×10^8
Rear Wing:	1.9×10^6	2.26×10^4

Figure 9.4.1 shows the shear and bending moment distributions along both wings. Notice that at the wing joint the front wing stresses will be much lower than that of an unsupported wing. This brace will be especially helpful during ground operation when the bottom skin is usually experiencing dangerous compressive stresses. Also deflection of the fuel-filled wing is greatly reduced due to the rear wing brace.

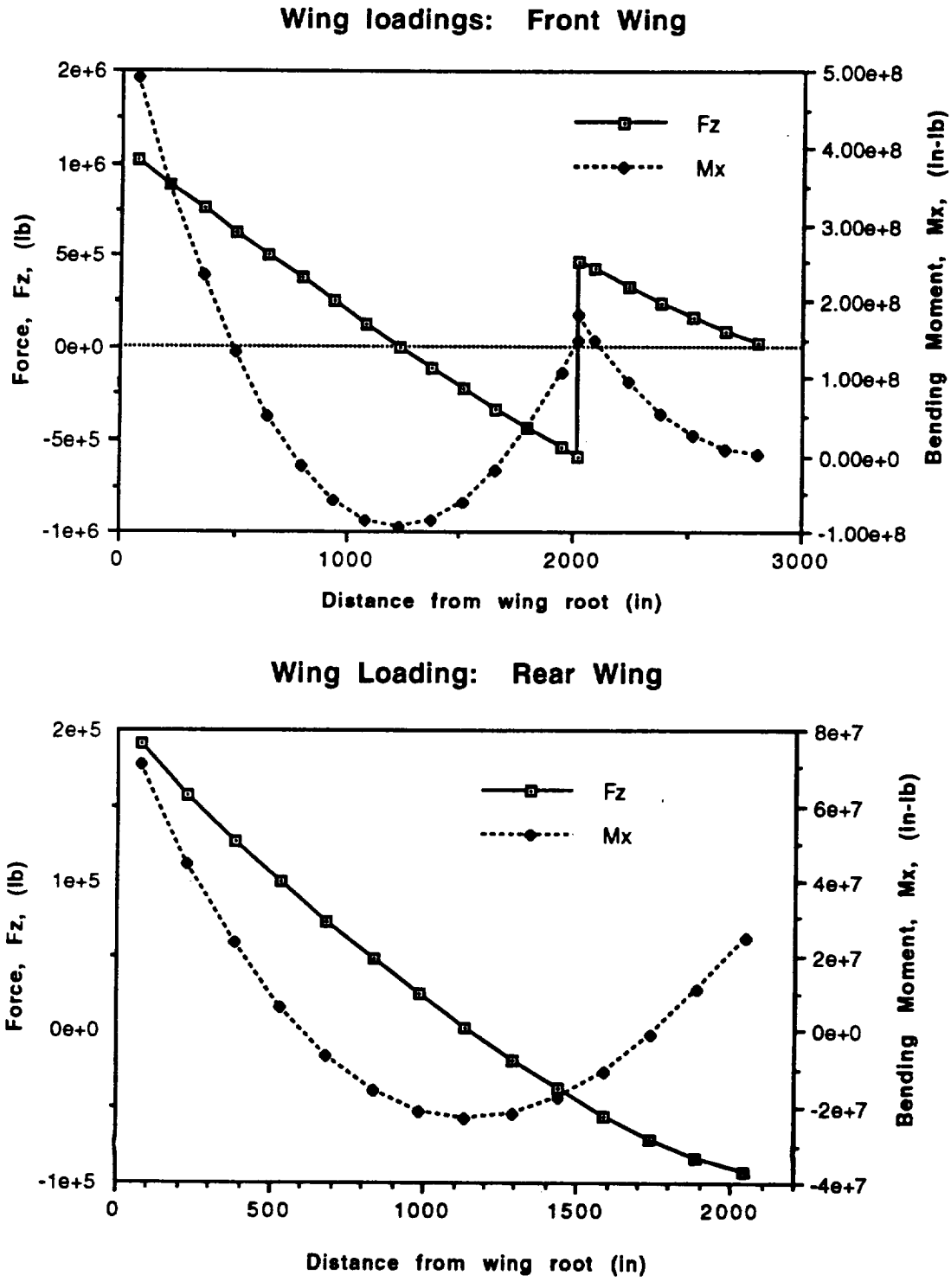

Figure 9.4.1 - Shear and Bending Moment

Figure 9.4.2 illustrates the wing box. As can be seen, the material in the spars is concentrated in the upper front and the lower rear corners. The wing box contains 65 percent of the overall wing chord. The spars are extruded graphite epoxy as are the stringers. All of the attachments in the diagram are bonded with adhesives i.e. no rivets, or other stress inducing discontinuities. Notice also that the ribs run perpendicular to the leading edge. This has the effect of requiring less material, because it lessens the amount of ribs needed. The 90 degree angle also makes for a stronger joint between the front spar and the ribs.

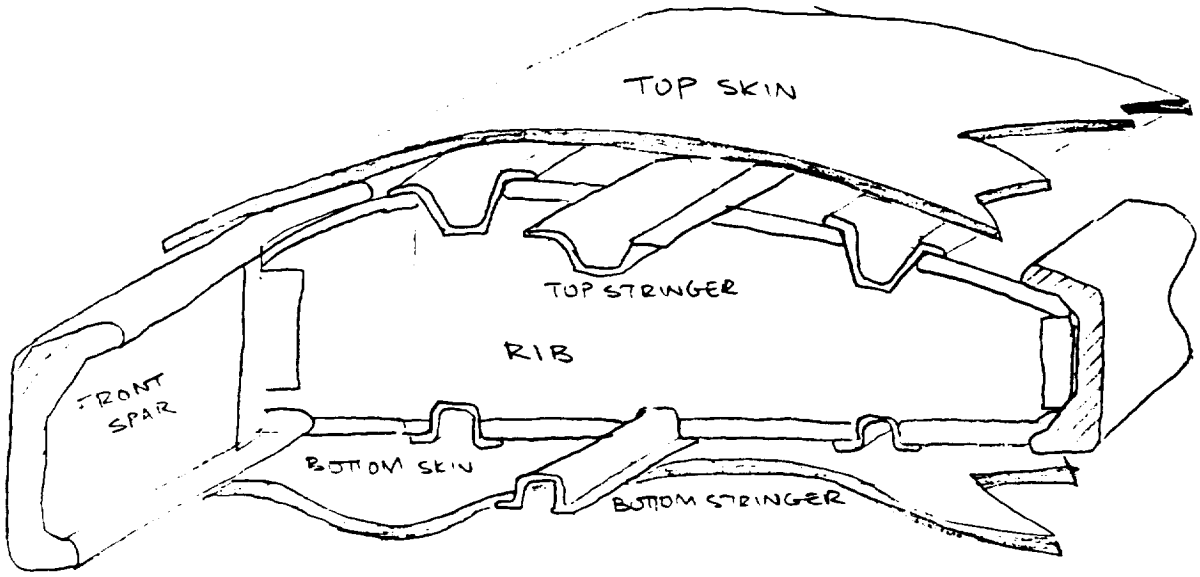

Figure 9.4.2 - Wing Box Cut Away

9.5. Fuselage Structure

The fuselage was designed as non-circular in order to facilitate the loading and unloading of the cargo. The goal was to lower the top of the cargo floor to five feet off the ground at the time of loading and unloading. A low floor

allows for a shorter ramp, a smaller door, more accessibly in remote locations (where K loaders may not always be available), and ease of boarding and deboarding of troops.

The top 210 degrees of fuselage is in fact circular, however at the point of junction with the floor structure, the walls begin to curve in to a flattened elliptical shape on the bottom as seen in figure 9.5.1. Thus the attachment of the floor at this point helps to handle the stresses by acting in tension to contain the ballooning pressure effect.

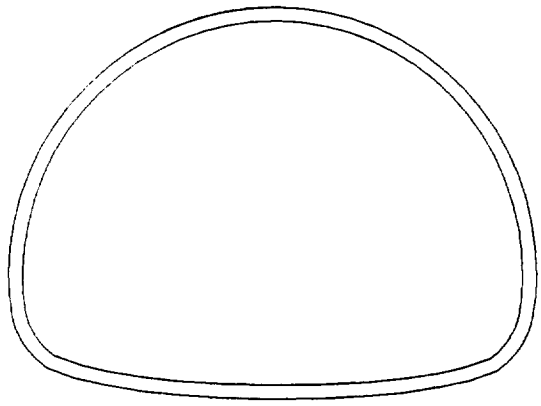

Figure 9.5.1 - Flattened Elliptical Shape

The fuselage structure itself is entirely composite. The skin is a thin ten layer 90,0,+45,-45,90 Graphite Epoxy shell. Attached to the shell is an isogrid with 6 inch deep spars at 60-60-60 degree angles, thus creating a complete indeterminate fail safe structural frame composed of eight inch isometric triangles (see figure 9.5.2). One of the spar directions runs parallel to the fuselage to stiffen it in the longitudinal direction, the others act against twisting created by the tail and uneven wing loading. The grid works as a whole to distribute loading throughout its members. The grid spar depth was determined in the

following manner: The fuselage was treated as a hollow tube. Forces and moments acting on the fuselage from cargo loading, wing loading, and maneuver loads were determined using JWOPT and weight and balance calculations. A shear-moment diagram was made for a worst case loading scenario of maximum bending in a 2.5g maneuver. With worth case scenario known, a program was written to optimize the moment of inertia of the fuselage longitudinal spars. Giving the spars a set thickness of 0.125 inches, gave a spar depth of approximately six inches and spacing of approximately 11 inches. The bending criteria was more rigorous than the twisting criteria and thus stresses in the fuselage due to twisting were more than compensated for.

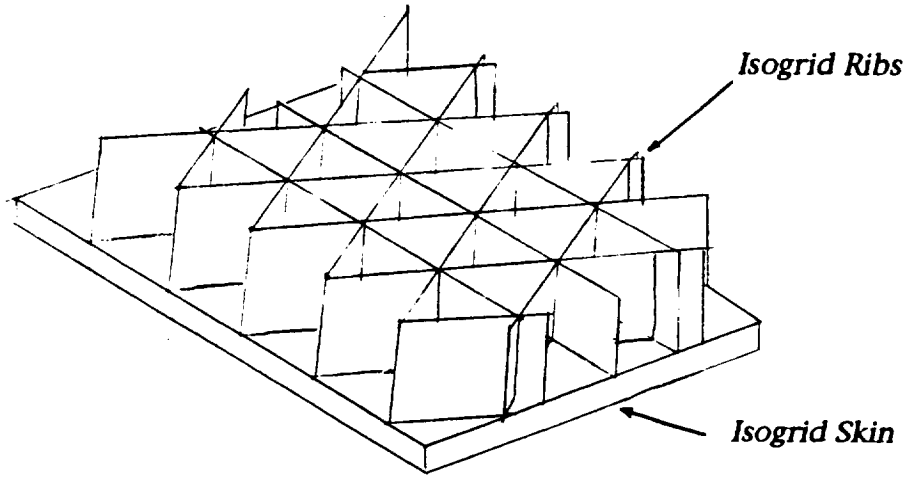

Figure 9.5.2 Isogrid Structure

DRAG

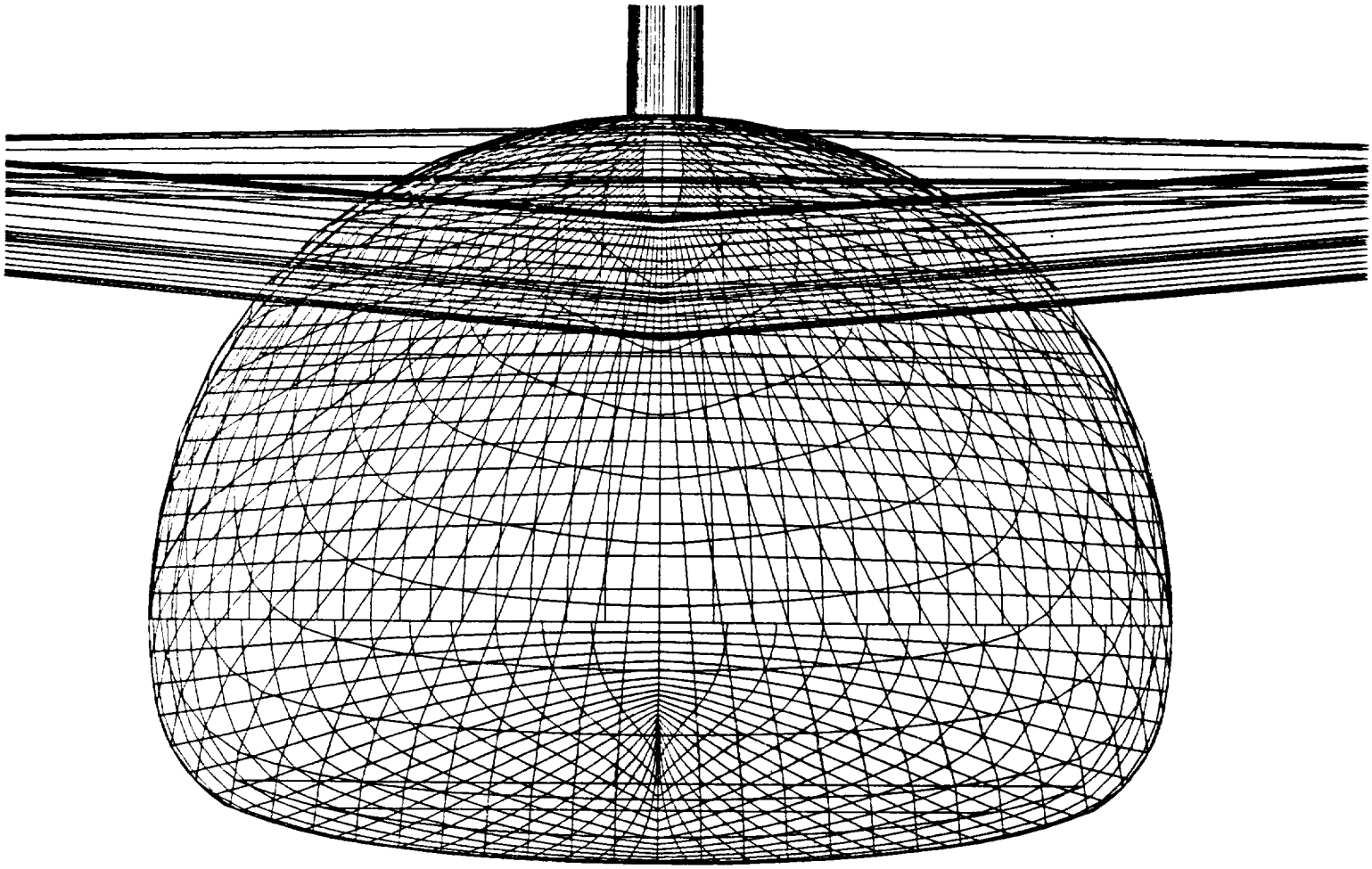

10. DRAG

In order to understand and verify the performance of the *Cetaceopteryx*, a drag estimation was conducted in the initial sizing of the aircraft and drag polars were calculated for takeoff, landing, and cruise.

The wetted areas shown in Table 10.0.1 were used to calculate the parasite drag for the different components of the aircraft exposed to the free stream.

Table 10.0.1 Wetted Areas (ft^2)

Fuselage	19200
Vertical Stabilizer	4300
Horizontal Stabilizer	5800
Wings	16700
Canard	1750
Pylons, Nacelles, etc.	9600
Total Wetted Area	57300

The *Cetaceopteryx* will be flying at a subsonic speed of mach 0.78. In this subsonic flight the induced drag was calculated using an Oswald efficiency factor of 1.03. This number was based on numbers found in Reference 11. In Figure 10.0.1 the theoretical span-efficiency factor for joined wing with or without symmetric inclined winglets is shown for several cases. It can be seen that as the height (h) increases, the span efficiency factor (e) increases. The Cetaceopteryx has a h/b value of 0.164. This results in a span efficiency factor of 1.03. The drag polar for the various flight configurations are shown in Figure 10.0.2.

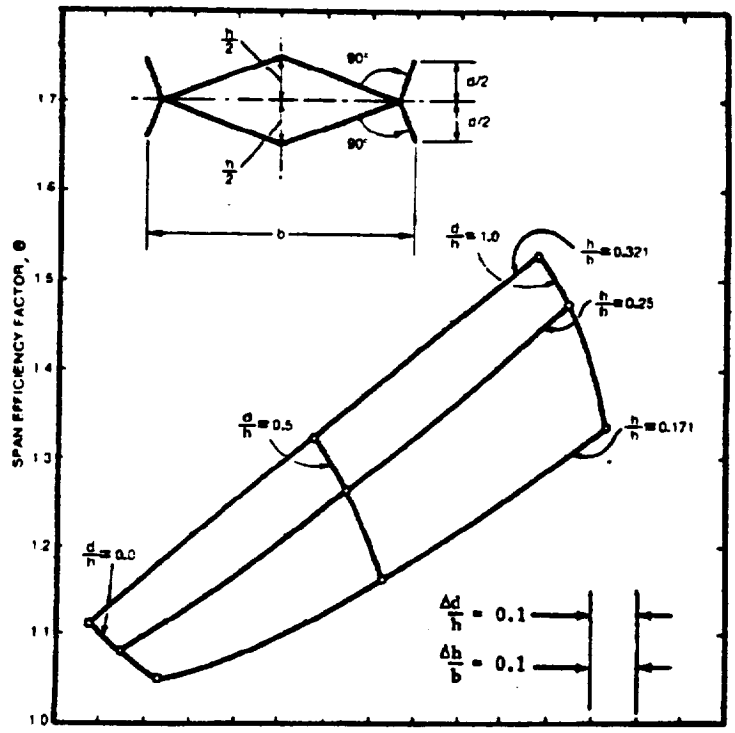

Figure 10.0.1 - Span Efficiency

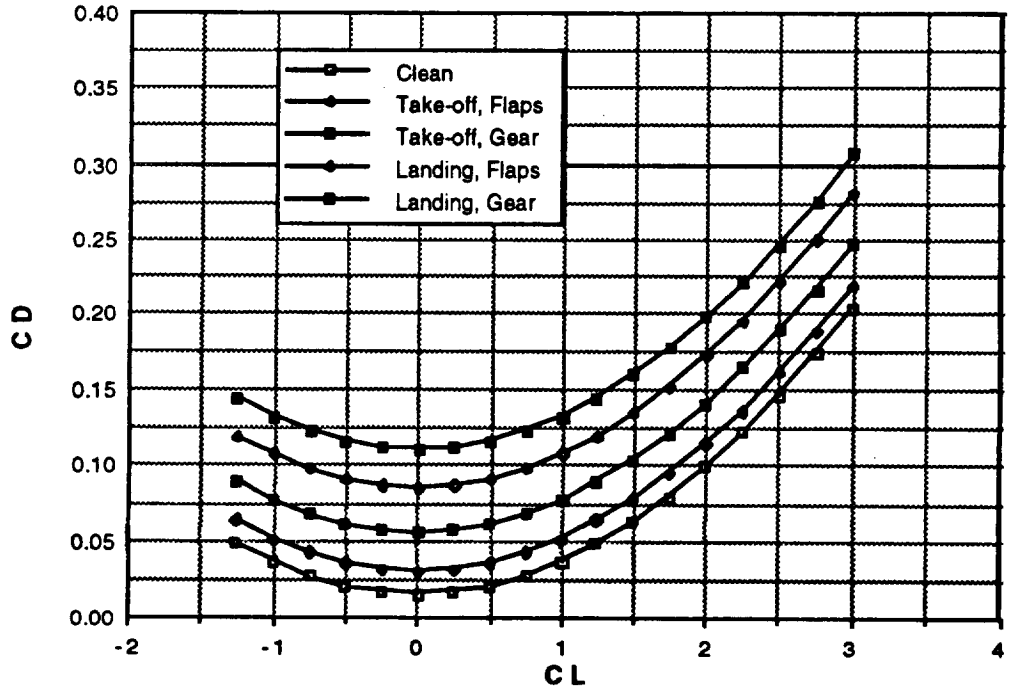

Figure 10.0.2 - Drag Polars

From these drag polar the attainable L/D maximum values were calculated for the aircraft and compared to the maximum L/D values required. The lift to drag ratios required for the various flight conditions are shown in Table 10.0.2.

Table 10.0.2 Lift to Drag Ratios Required

Segment	L/D
Climb	25.0
Cruise	29.0
Loiter	25.0

The highest value of L/D occurs at cruise. This value of L/D may seem high but according to the drag polar, at cruise, the aircraft is obtaining a maximum L/D value of 30. But at the cruise C_L of 0.4 , according to Figure 10.0.2, the Cetaceopteryx will only be achieving an L/D of 25. This L/D is lower than the required L/D at cruise but this value does not take into account any kind of laminar flow control or drag reduction system. In order to achieve this required L/D value, a drag reduction system was chosen, selective suctioning[34], that would decrease the aircraft's skin friction drag by up to 60%. Since the skin friction drag is half of the Cetaceopteryx's total drag, the total drag would be reduced by up to 30%. This reduction would give the Cetaceopteryx a cruise L/D of 31. This value is well above the L/D value needed for cruise.

STABILITY & CONTROL

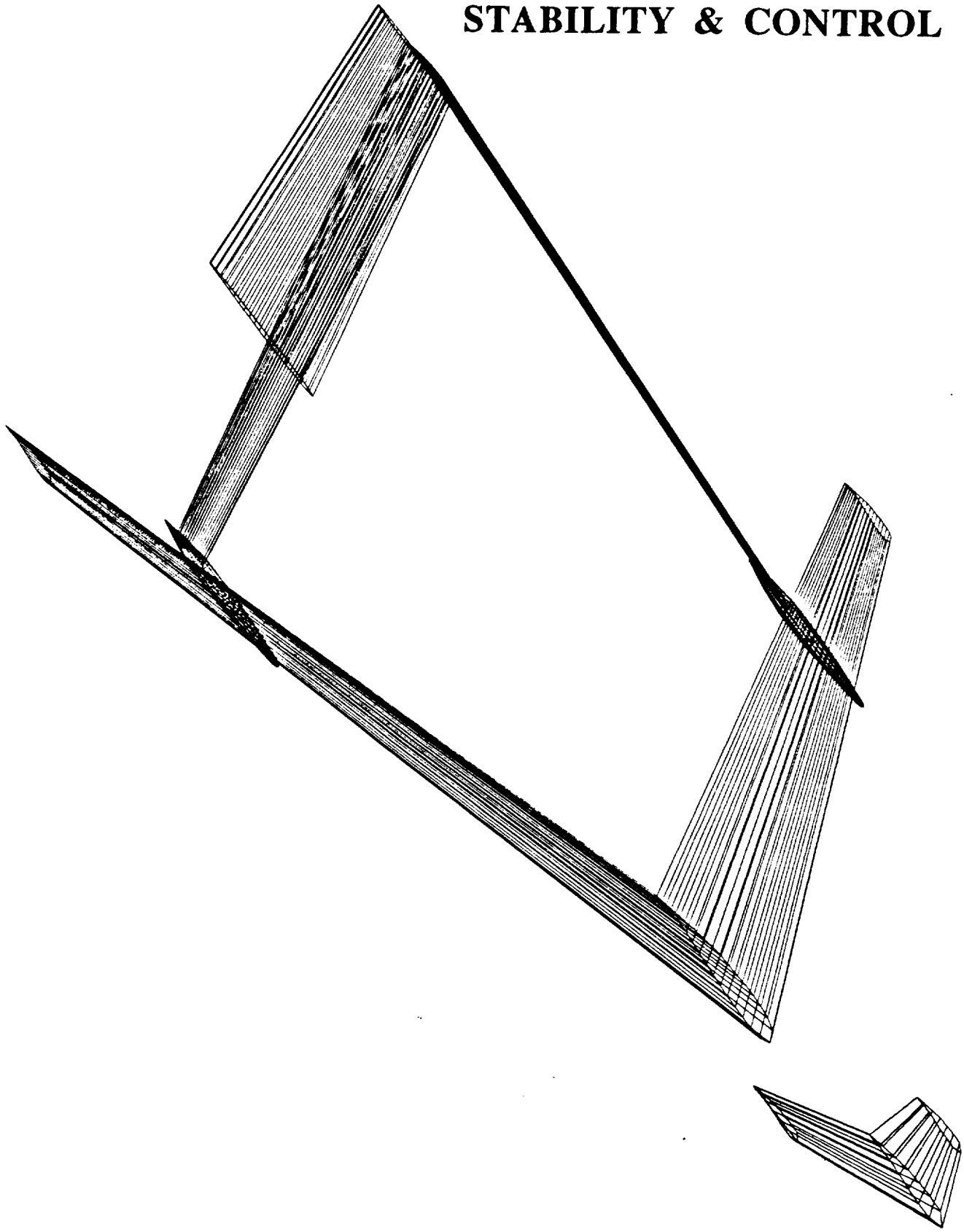

11. STABILITY AND CONTROL

11.1. Center of Gravity Excursion

The CG Excursion plot is shown in Figure 11.1.1. One of the most unusual features is the large aft shift in CG when fueling *Cetaceopteryx*. These CG shifts are inconsequential to the stability considerations, since they will only occur while the aircraft is parked on the tarmac. As a result, *Cetaceopteryx* has an operational constraint in that it may not fly fuel ferry missions, i.e., it cannot fly with fuel and no cargo. During flight, the CG travels from the point labeled "(to)" to the one labeled "(land)", a shift of about 1-1/2 feet, or 5% of the m.a.c.

11.2. Static Stability

How well an airplane flies and how easily it can be controlled are the subjects studied in aircraft stability and control. Stability is the tendency of the airplane to return to its equilibrium position after it has been disturbed. Stability is a requirement for all airplanes and can be satisfied in an open or closed loop manner. If stability is satisfied "open loop", it is referred to as "inherent stability" and if it is satisfied "closed loop", it is referred to as "de facto stability". Although airplanes with little or no inherent aerodynamic stability can be flown, they are unsafe to fly, unless they are provided artificial stability by way of an electromechanical device called a stability augmentation system (SAS). Static stability is the initial tendency of the vehicle to return to its equilibrium state after a disturbance, whereas, dynamic stability is

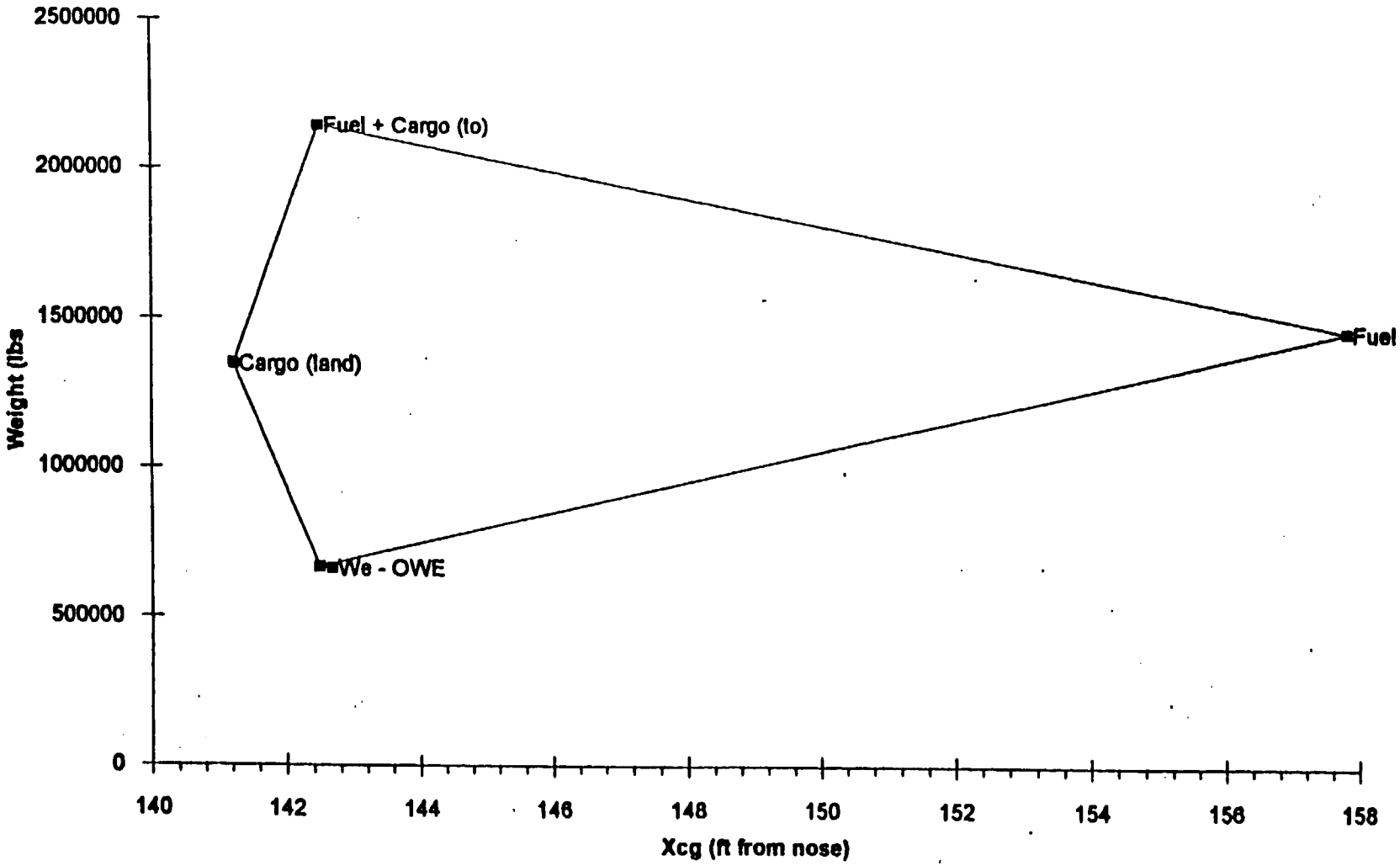

Figure 11.1.1 - Cetaceopteryx CG Excursion Diagram

concerned with the time history of the motion of the vehicle after it is disturbed from its equilibrium point.

As determined from initial sizing by methods presented in Reference 6, *Cetacepteryx* is slightly unstable for longitudinal and lateral axes with static margin = 0.007. The empenage sizing of the aircraft has been used as the basis for stability derivatives calculations in Table 11.2.1 for longitudinal, and Table 11.2.2 for lateral derivatives. Since *Cetaceopteryx's* mission is dominated by cruise, the stability derivatives have been calculated for this phase of flight. Geometric and aerodynamic characteristics of the aircraft are the basis for these stability derivatives which determine the static and dynamic stability and control behavior of *Cetaceopteryx*. The sensitivity of the aircraft's response to various forces and perturbations during flight depends on the magnitude of these derivatives. As the magnitude of these derivatives approaches zero, the less sensitive aircraft would be to that particular force. As can be seen, *Cetaceopteryx* is most sensitive to pitch rate for longitudinal stability and yaw rate for lateral stability.

Table 11.2.1 - Longitudinal Stability Derivatives

Longitudinal	Cruise
$C_{D\,o}$	0.149
$C_{D\,u}$	0.060
$C_{D\,\alpha}$	0.003
$C_{D\,\dot{\alpha}}$	0.000
$C_{D\,q}$	0.000
$C_{D\,ih}$	0.005
$C_{D\,\delta e}$	0.015
$C_{L\,o}$	0.510
$C_{L\,u}$	0.430
$C_{L\,\alpha}$	0.150
$C_{L\,\dot{\alpha}}$	0.000
$C_{L\,q}$	0.694
$C_{L\,ih}$	0.004
$C_{L\,\delta e}$	0.117
$C_{m\,o}$	-0.660
$C_{m\,u}$	0.000
$C_{m\,Tu}$	0.004
$C_{m\,T\alpha}$	0.000
$C_{m\,\alpha}$	-0.236
$C_{m\,\dot{\alpha}}$	-0.002
$C_{m\,q}$	-1.645
$C_{m\,ih}$	0.002
$C_{m\,\delta e}$	0.006

Table 11.2.2 - Lateral Stability Derivatives

Lateral - Directional	Cruise
$C_{y\beta}$	-0.284
$C_{y\dot{\beta}}$	-0.001
C_{yp}	-0.004
C_{yr}	0.026
$C_{l\beta}$	-0.002
$C_{l\dot{\beta}}$	0.000
C_{lp}	-0.042
C_{lr}	0.817
$C_{n\beta}$	0.004
$C_{n\dot{\beta}}$	0.000
C_{np}	-0.301
C_{nr}	-0.019

11.3. Dynamic Stability

11.3.1. Longitudinal

The longitudinal motion of *Cetaceopteryx* (control fixed), disturbed from its equilibrium flight condition is characterized by two oscillatory modes of motion. One mode is lightly damped and has a long period called the phugoid mode and the second mode is more damped and has a very short period; it is appropriately called the short-period. Of the two characteristic modes, the short- period

mode is the most important. If this mode has a high frequency and is heavily damped, then the aircraft will respond rapidly to an elevator input without any undesirable overshoot. When the short-period mode is lightly damped or has a relatively low frequency, the aircraft will be difficult to control and, in some cases, may even be dangerous to fly. As can be seen from Table 11.2.1 the short-period mode of *Cetaceopteryx* has a relatively low frequency $w_{n\,p}$ = 0.069 rad/s.

The phugoid or long-period mode occurs so slowly that the pilot can easily negate the disturbance by small control movements. Even though the pilot can easily correct for the phugoid mode, it would become extremely fatiguing if the damping were too low. For this mode, *Cetaceopteryx* shows wsp = 0.68 rad/s, which is a very low damping frequency. Therefore, the need for an autopilot system arises.

Table 11.3.1 - Longitudinal Literal Factors

Literal Factors	Cruise
Phugoid natural frequency - ω_p	0.069 rad/s
Phugoid damping ratio - ζ_p	0.21
Short period natural frequency ω_{sp}	0.68 rad/s
Short period damping ratio - ζ_{sp}	0.4

11.3.2. Lateral

There are two potential lateral dynamic instabilities of interest to *Cetaceopteryx's* designers: directional divergence and the so-called Dutch roll oscillation. The mentioned literal factors have been calculated and presented in Table 11.2.2.

Directional divergence can occur when the aircraft does not possess directional or weathercock stability. Therefore, if the aircraft is disturbed from its equilibrium state it will tend to rotate to ever-increasing angels of sideslip. However, since *Cetaceopteryx* has adequate dihedral, the motion can occur without any significant change in bank angle. The period for this mode is 2.1 seconds. This characteristics could certainly be improved with the implementation of a stability augmentation system (SAS).

Spiral divergence is a nonoscillatory divergent motion which can occur when directional stability is large and lateral stability is small. When disturbed from equilibrium, the aircraft enters a gradual spiraling motion. The spiral becomes tighter and steeper as time proceeds and can result in a high-speed spiral dive if corrective action is not taken.

The Dutch roll oscillation is a coupled lateral-directional oscillation which can be quite objectionable to pilots and passengers. The motion is characterized by a combination of rolling and yawing oscillations which have the same frequency but are out of phase with one another. The period can be of the order of 3 to 16 seconds, so that if the amplitude is appreciable the motion can be very annoying. The Dutch roll frequency for *Cetaceopteryx* is $W_{DR} = 0.12$

rad/s with a time to double amplitude of 16.1 seconds. Although these parameters are within the range of pilot satisfaction, they could be improved with implementation of a stability augmentation system.

Following are the *Cetaceopteryx's* literal factors calculated by using the longitudinal and lateral approximation methods presented in Reference 38.

Table 11.2.2 - Lateral Literal Factors

Literal Factors	Cruise
Dutch roll natural frequency - ω DR	0.12 rad/s
Dutch roll damping ratio - ζ DR	0.36
Time to double amplitude (Dutch roll) - t 2	16.1 sec
Roll damping ratio - ζ roll	0.48
Time to double amplitude (roll) - t 2	1.5 sec

11.4. Handling Qualities

Reference 37 defines the following terminology as the flight phase categories:

Nonterminal Flight Phase:

Category A

Nonterminal flight phases that require rapid maneuvering, precision tracking, or precise flight-path control. Included in the category are air-to-air combat ground attack, weapon delivery/launch, aerial recovery, reconnaissance, in-flight

refueling (receiver), terrain-following, antisubmarine search, and close-formation flying.

Category B

Nonterminal flight phases that are normally accomplished using gradual maneuvers and without precision tracking, although accurate flight-path control may be required. Included in the category are climb, cruise, loiter, in-flight refueling (tanker), descent, emergency descent, emergency deceleration, and aerial delivery.

Terminal Flight Phases

Category C

Terminal flight phases are normally accomplished using gradual maneuvers and usually require accurate flight-path control. Included in this category are take-off, approach, wave-off/go-around and landing.

Classification of airplanes are as follows:

Class I

Small, light airplanes, such as light utility, primary trainer, and light observation craft

Class II

Medium-weight, low-to-medium maneuverability airplanes, such as heavy utility/search and rescue, light or medium transport/cargo/tanker, reconnaissance, tactical bomber, heavy attack and trainer for Class II

Class III

Large, heavy, low-to-medium maneuverability airplanes, such as heavy transport/cargo/tanker, heavy bomber and trainer for Class III

Class IV

High-maneuverability airplanes, such as fighter/interceptor, attack, tactical reconnaissance, observation and trainer for Class IV

Flying qualities are specified in terms of three levels:

Level 1

Flying qualities clearly adequate for the mission flight phase.

Level 2

Flying qualities adequate to accomplish the mission flight phase, but some increase in pilot workload or degradation in mission effectiveness, or both, exists.

Level 3

Flying qualities such that the airplane can be controlled safely, but pilot workload is excessive or mission effectiveness is inadequate, or both. Category A flight phases can be terminated safely, and category B and C flight phases can be completed.

With the aforementioned definitions, the flying qualities of the *Cetaceopteryx*, a Class III Category B and C aircraft, can be summarized in Table 11.2.4.

Table 11.2.4 - *Cetaceopteryx's* Handling Quality

Modes of motion	Category	Level
Long Period Mode (Phugoid)	B C	Level 1 Level 1
Short Period Mode	B C	Level 1 Level 1
Dutch Roll Mode	B C	Level 2 Level 2
Roll Mode	B C	Level 1 Level 1

As can be seen in this table, even though with *Cetaceopteryx's* slight instability which can easily be compensated for by rearranging the cargo, the aircraft has demonstrated good handling qualities for all modes of motion except for the dutch roll mode. The deficiency in this mode can be improved to a level 1 handling quality as mentioned earlier, with a stability augmentations system.

Although *Cetaceopteryx* illustrates good handling qualities, Hydra design team feels that it is advantageous to incorporate a fly-by-wire system in the aircraft's avionics system for the following reasons:

1) More efficiency during cruise which translates into better specific fuel consumption

2) Global positioning system (GPS) capability

3) Decrease in pilot's workload.

SYSTEMS LAYOUT

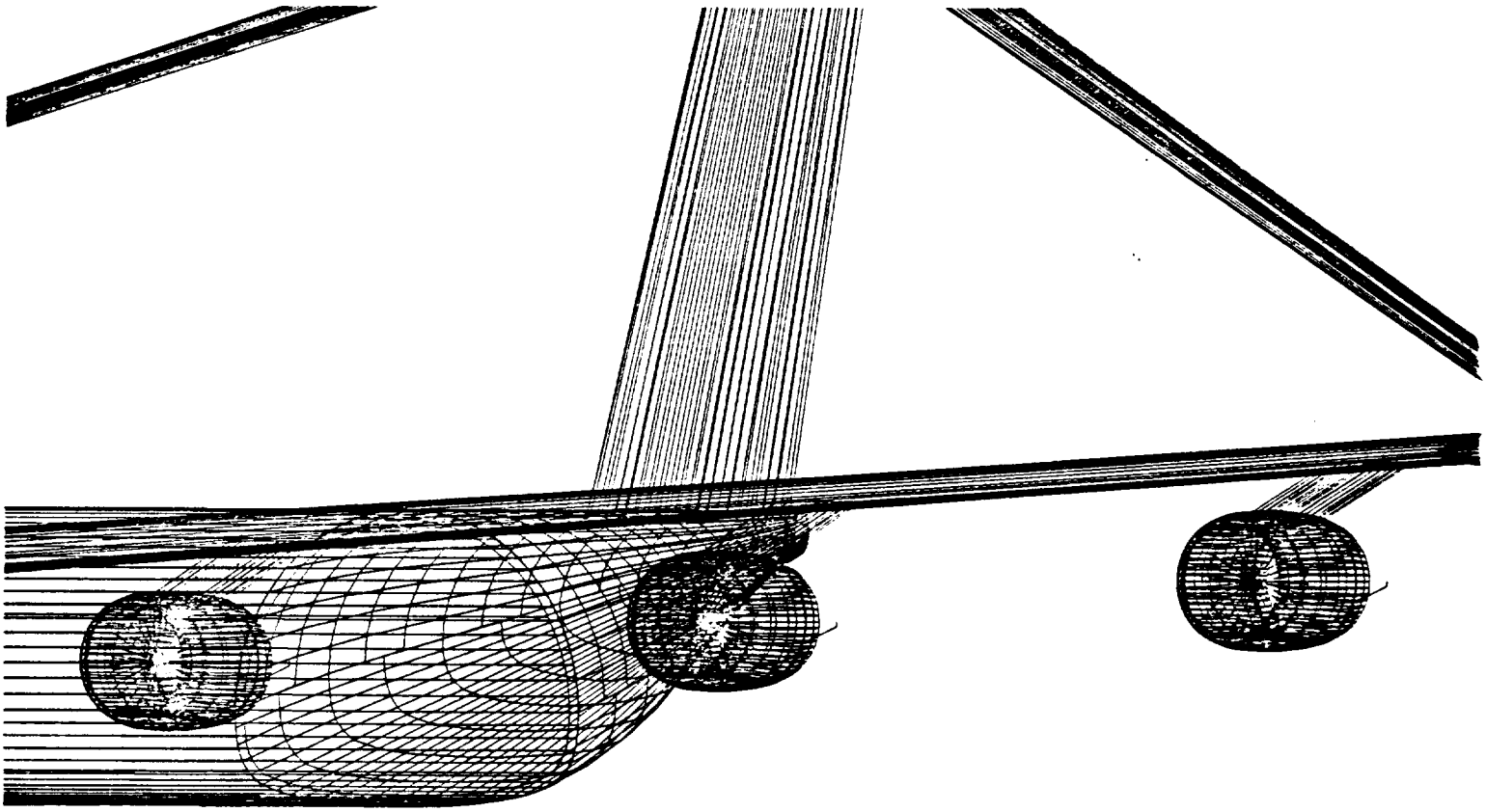

12. SYSTEMS LAYOUT

Since the *Cetaceopteryx* is such a large aircraft, finding the space for the various aircraft systems is not as crucial as it is for smaller aircraft. Therefore, the systems needed and the general areas where they will be placed are discussed.

There is a large area that will be used under the cockpit of approximately 20,000 ft^3. Here the radome, avionics and electrical systems will be stored. In the rear of aircraft, in the tail cone, there is also additional space that will be used for the APU and waste systems.

The hydraulic lines and other electrical systems will be ran through the spaces in the wings and throughout the shell of the fuselage. The hydraulic lines were laid out in such a way that damage or failure in one system would not effect the others.

Above the cargo section behind the cockpit will be the environmental control system. The entire aircraft will be pressurized, including the cargo bay. The air conditioner and heater will only be used in the cockpit and troop section during ground operations. Both the front and rear of the aircraft will be open during loading and unloading. Therefore, it would be very inefficient to try and control the temperature in the cargo bay. However, when the aircraft is in flight, the entire structure will be heated if need be.

C-2

COST ANALYSIS

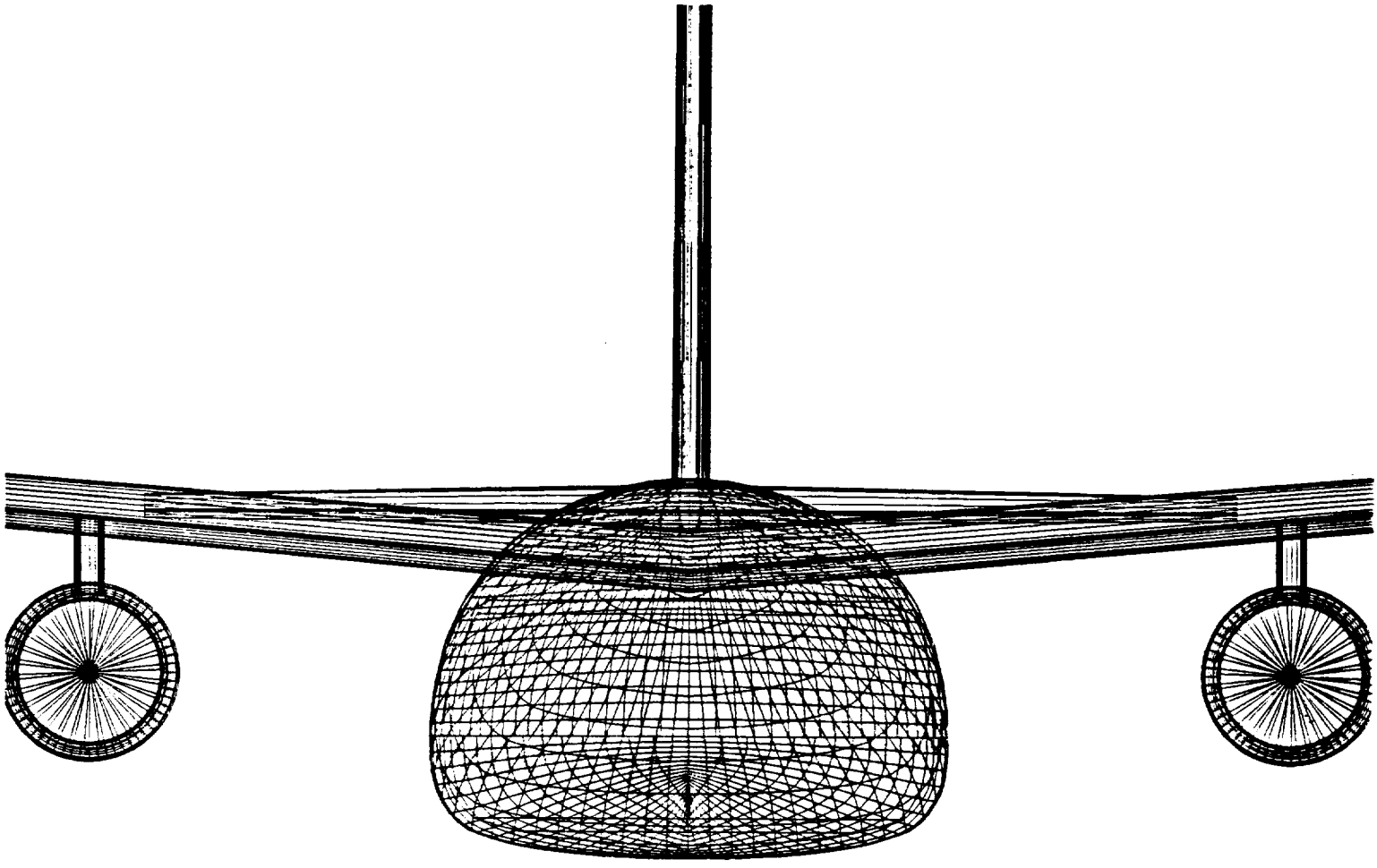

13. COST ANALYSIS

Throughout the design of the *Cetaceopteryx*, because it is a military plane and because it is a plane that has specific missions that have never been designed for before, the plane is using advance technology and materials. The Cetaceopteryx cost analysis is scaled to 1993 dollars using a cost escalation factor and a price of 1.07 billion per aircraft was computed for 50 military transports. Though this price may seem high, it must be remembered that this plane is using advance technology and that it is doing the job of four McDonnell Douglas C-17's. All of the analysis was done using the data from the primary mission.

13.1. Life Cycle Cost

The life cycle cost is broken down into four sections.

1. Research, Development, Test and Evaluation
2. Acquisition Cost
3. Maintenance Cost
4. Disposal Cost

Table 13.1.1 shows the breakdown and total of the life cycle cost.

Table 13.1.1 Life Cycle Cost

	1993 Dollars in Billions
RDT and E Cost	12.98
Acquisition Cost	215.63
Operating Cost	26.89
Disposal Cost	2.58
Life Cycle Cost	258.08

13.2. Research, Development, Test and Evaluation

The research, development, test and evaluation (RDT & E) cost is based on a production of six aircraft, which does not include the 50 production aircraft. Table 13.2.1 shows the costs of the individual sections which total the RDT and E.

Table 13.2.1 RDT and E Cost

	1993 Dollars in Billions
Airframe Engineering and Design	0.906
Development Support and Testing	0.363
Flight Test Airplanes Cost	6.14
Flight Test Operations Cost	0.381
Test and Simulation Facilities Cost	2.60
Ten Percent Profit	1.30
Ten Percent Financing	1.30
Total RDT and E Cost	12.990

13.3. Acquisition Cost

The acquisition cost for the Cetaceopteryx is shown in Table 13.3.1. The acquisition cost is broken down into several sections. These sections include the Airframe Engineering and Design Cost, The Production Cost, Production Flight and Test Operations and Cost of Financing the Manufacturing Program.

Table 13.3.1 Acquisition Cost

	1993 Dollars in Billions
Manufacturing Cost	
Airframe Engin. and Design	0.451
Airplane Production	175.93
Production Flight Test Oper.	0.043
Financing (Ten percent)	19.60
Subtotal	196.03
Profit (Ten percent)	19.60
Total Acquisition Cost	215.63

13.4. Operating Cost

The Cetaceopteryx operating cost is broken down in seven categories: Fuel Cost, Crew Salaries, Spares Cost, Consumable Materials cost, Indirect Personnel Cost, Depot Cost, and a Miscellaneous Cost. These costs are shown in Table 13.4.1.

Table 13.4.1 Operating Cost

	1993 Dollars in Billions
Fuel, Oil and Lubricants	6.67
Direct Personnel (Aircrew and Maint.)	5.72
Spares Cost	3.50
Consumable Materials Cost	0.518
Indirect Personnel Cost	4.30
Depot Cost	5.38
Miscellaneous Cost	0.807
Total Operating Cost	26.89

The fuel cost was calculated using 36.3 aircraft in service with each aircraft carrying 137,069 gallons of fuel at 0.75$/gal. The crew salaries were estimated knowing there would be eight crew members. The salary, because it is a military aircraft was averaged at $35,000 per year.

13.5. Disposal Cost

The disposal cost was based on a twenty year life of each plane. The disposal cost is broken down to:

1. Temporary storage

2. raining of liquids and disposal thereof.

3. Disassembly of engines and certain systems.

4. Cutting up of airframe and disposal of the resulting material.

The disposal cost came to be 2.58 billion dollars.

CONCLUSION

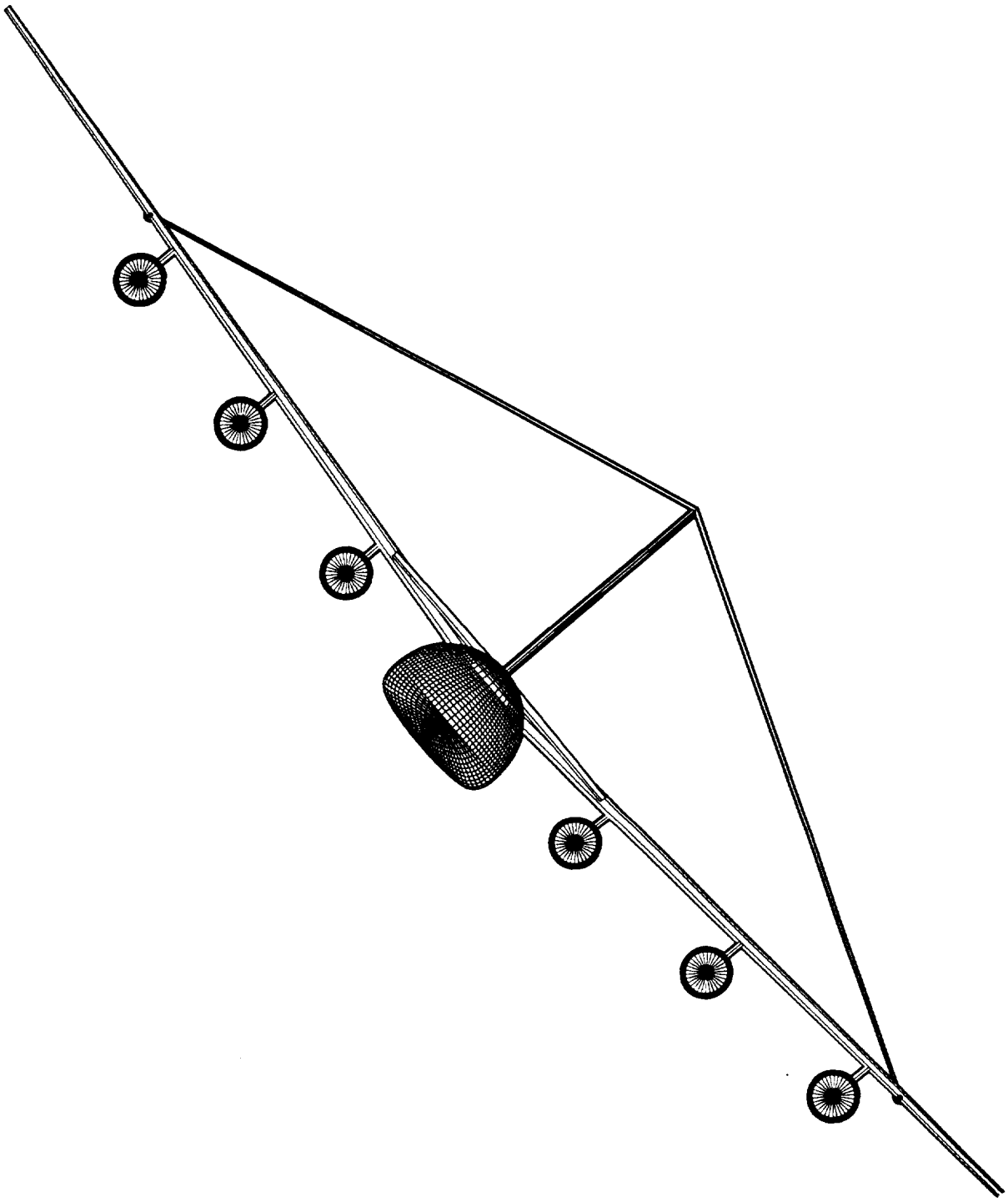

14. CONCLUSION

The *Cetaceopteryx* provides a unique solution to transporting a large volume of payload to any point on the globe without refueling. During periods of armed conflict or international emergencies, this type of aircraft which can transport cargo and troops to any location in the world is of great importance. This aircraft will be cruising at a mach of 0.78 and has the capability of carrying four times the cargo of the McDonnell Douglas C-17.

Due to the unique capabilities of the aircraft, the *Cetaceopteryx* had to implement new design techniques and technology. The *Cetaceopteryx* will not begin service until the year 2015, therefore certain assumptions were made such as the wide use of composites in the structure of aircraft and the achievement of higher amounts of thrust from the GE-90 engine. The joined-wing configuration of the *Cetaceopteryx* and its composite structure allows the aircraft to have a much lighter weight than a conventional design, and possesses many aerodynamic and structural advantages.

The *Cetaceopteryx* is a unique combination of advance design and advance technology resulting in an aircraft with capabilities of no other. With a production of fifty aircraft, not including the experimental aircraft, each transport aircraft will cost the nation 1.07 billion (1993) dollars.

REFERENCES

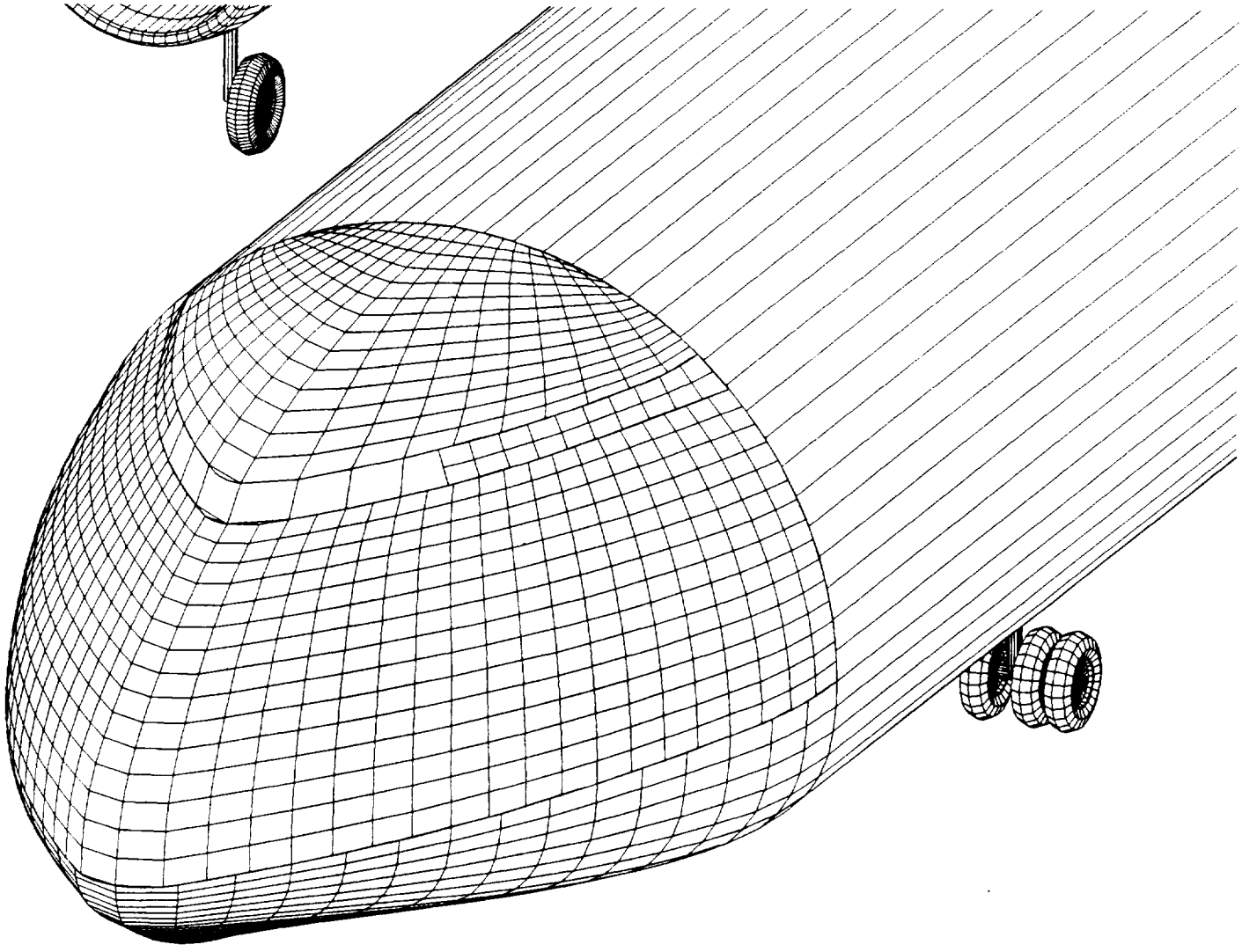

15. REFERENCES

1. Anon., RFP for AIAA Student Competition, 1992/1993 AIAA/General Dynamics Corporation Team Aircraft Design Competition.

2. Roskam, J., Airplane Design: Part I, Preliminary Sizing of Airplanes, Roskam Aviation and Engineering corporation, Ottawa, Kansas, 1985.

3. Cliff, S. E., Kroo, I. M., and Smith, S. C., The Design of a Joined-Wing Flight Demonstrator Aircraft, AIAA/AHS/ASEE Aircraft Design, Systems and Operations Meeting, AIAA 87-2930, St. Louis, Missouri, 1987.

4. Wolkovitch, J., The Joined Wing: An Overview, AIAA 23rd Aerospace Sciences Meeting, AIAA 85-0274, Reno Nevada, 1985.

5. Hajela, P., Weight Evaluation of Joined Wing Configuration, NASA Contractor Report 166592, 1984.

6. Wolkovitch, J., Joined-Wing Research Airplane, AIAA/AHS/ASEE Aircraft Design Systems and Operations Meeting, AIAA-84-2471, San Diego, CA, 1984.

7. Wolkovitch, J., Joined Wing Technology, ACA Industries, Inc., Torrance, CA, 1984.

8. Roskam, J., Airplane Design: Part VI, Preliminary Calculation of Aerodynamic, Thrust and Power Characteristics, Roskam Aviation and Engineering corporation, Ottawa, Kansas, 1985.

9. Roskam, J., Airplane Design: Part V, Component Weight Estimation, Roskam Aviation and Engineering Corporation, Ottawa, Kansas, 1985.

10. Currey, N., Aircraft Landing Gear Design: Principles and Practices, AIAA Education Series, Washington D.C., 1988.

11. Wolkovitch, J., Principles of the Joined Wing, Engel Engineering Company Report No. 80-1, 1980.

12. Roskam, J., Airplane Design: Part II, Preliminary Configuration Design and Integration of the Propulsion System, Roskam Aviation and Engineering corporation, Ottawa, Kansas, 1985.

13. Roskam, J., Airplane Design: Part III, Layout Design of Cockpit, Fuselage, Wing and Empennage: Cutaways and Inboard Profiles, Roskam Aviation and Engineering corporation, Ottawa, Kansas, 1985.

14. Roskam, J., Airplane Design: Part IV, Layout Design of Landing Gear and Systems, Roskam Aviation and Engineering corporation, Ottawa, Kansas, 1985.

15. Roskam, J., Airplane Design: Part VII, Determination of Stability, Control and Performance Characteristics: FAR and Military Requirements, Roskam Aviation and Engineering corporation, Ottawa, Kansas, 1985.

16. Roskam, J., Airplane Design: Part VIII, Airplane Cost Estimation and Optimization: Design, Development Manufacturing and Operating, Roskam Aviation and Engineering corporation, Ottawa, Kansas, 1985.

17. Mattingley, J., Heiser, W., and Daley, D., Aircraft Engine Design.

18. Anon., General Electric: The Leading Edge, Fall 1992.

19. Anon., General Electric: Competitive Advantage, GE90.

20. Foch, R., and Toot, P., Flight Testing of the Low Altitude/Airspeed Unmanned Research Aircraft (LAURA), AIAA/SFTE/DGLR/SETP Fifth Biannual Flight Test Conference, AIAA 90-1262, Ontario, CA, 1990.

21. Gallman, J. W., Kroo, I. M., and Smith, S. C., Design Synthesis and Optimization of Joined-Wing Transports, AIAA/AHS/ASEE Aircraft Design, Systems and Operations Conference, AIAA 90-3197, Dayton, OH, 1990.

22. Burkhalter, J. E., Key, M. K., and Spring, D. J., Downwash for Joined-Wing Airframe with Control Surface Deflections, Journal of Aircraft, Vol. 29, No. 3, May-June 1992.

23. Brooks, C. W. Jr., Cluckey, P. G., Harris, C. D., Stack, J. P., The NASA Langley Laminar-Flow Control Experiment on a Swept, Supercritical Airfoil, Evaluation of Initial Perforated Configuration, NASA Technical Memorandum 4309, 1992.

24. Kendall, E. R., The Aerodynamics of Three-Surface Airplanes, Gates Learjet Corporation, Wichita, Kansas.

25. Wolkovitch, J., Applications of the Joined Wing, International Aerospace Symposium Nagoya, 1989.

26. Hashimoto, M., Hirose, N., Ishikawa, M., and Ohnuki, T., Computational and Experimental Analysis of Joined-Wing Aerodynamics, ICAS-90-2.6.1, 1990.

27. Clyde, J., A., Transonic Design and Wind Tunnel Testing of a Joined Wing Concept, AIAA/AHS/ASEE Aircraft Systems Design and Operations Meeting, AIAA-84-2433, San Diego, CA, 1984.

28. Miura, H., Shyu, A. T., and Wolkovitch, J., Parametric Weight Evaluation of Joined Wings by Structural Optimization, AIAA/ASME/ASCE/AHS 26th Structures, Structural Dynamics and Materials Conference, Paper No. 85-0642-CP, Orlando, FL, 1985.

29. Shevell, R. S., Fundamentals of Flight, Prentice Hall, Englewood Cliffs, NJ, 1983.

30. Hoerner, S. F., Fluid-Dynamic Drag, Hoerner Fluid Dynamics, 1965.

31 Taylor, J. W. R., Jane's All The World Aircraft, Jane's Publishing Company, London England, 1990/91.

32. Abbott, I. H., and Von Doenhoff, A. E., Theory of Wing Sections, Dover Publications, Inc., New York, 1949.

33. Eppler, R., Airfoil Design and Data, Springer-Verlag Berlin, Heidelberg, 1990.

34. Gallman, J. W., and Kroo I., IWOPT - An Optimization and Analysis Program for Joined Wing and Conventional Aircraft Structures, Stanford University, 1988.